Journal Pre-proof

Use of Calcium Carbonate Nanoparticles in Production of Nano-Engineered Foamed Concrete

Md Azree Othuman Mydin, P. Jagadesh, Alireza Bahrami, Anmar Dulaimi, Yasin Onuralp Özkılıç, Mohd Mustafa Al Bakri Abdullah, Ramadhansyah Putra Jaya

PII: S2238-7854(23)01919-1

DOI: https://doi.org/10.1016/j.jmrt.2023.08.106

Reference: JMRTEC 8200

To appear in: *Journal of Materials Research and Technology*

Received Date: 2 June 2023

Revised Date: 31 July 2023

Accepted Date: 12 August 2023

Please cite this article as: Othuman Mydin MA, Jagadesh P, Bahrami A, Dulaimi A, Onuralp Özkılıç Y, Al Bakri Abdullah MM, Jaya RP, Use of Calcium Carbonate Nanoparticles in Production of Nano-Engineered Foamed Concrete, *Journal of Materials Research and Technology*, https://doi.org/10.1016/j.jmrt.2023.08.106.

Use of Calcium Carbonate Nanoparticles in Production of Nano-Engineered Foamed Concrete

Md Azree Othuman Mydin[1,*], P. Jagadesh[2], Alireza Bahrami[3,*], Anmar Dulaimi[4,5], Yasin Onuralp Özkılıç*[6], Mohd Mustafa Al Bakri Abdullah[7,8], Ramadhansyah Putra Jaya[9]

[1]School of Housing, Building and Planning, Universiti Sains Malaysia, Penang 11800, Malaysia; azree@usm.my

[2]Department of Civil Engineering, Coimbatore Institute of Technology, Tamil Nadu, 638 056, India; jaga.86@gmail.com

[3]Department of Building Engineering, Energy Systems and Sustainability Science, Faculty of Engineering and Sustainable Development, University of Gävle, 801 76 Gävle, Sweden alireza.bahrami@hig.se

[4]College of Engineering, University of Warith Al-Anbiyaa, Karbala, Iraq;

a.f.dulaimi@uowa.edu.iq

[5]School of Civil Engineering and Built Environment, Liverpool John Moores University, Liverpool L3 2ET, UK

[6]Department of Civil Engineering, Faculty of Engineering, Necmettin Erbakan University, Konya, Turkey; yozkilic@erbakan.edu.tr

[7]Centre of Excellence Geopolymer and Green Technology, Universiti Malaysia Perlis, Arau 01000, Perlis, Malaysia; mustafa_albakri@unimap.edu.my

[8]Faculty of Chemical Engineering and Technology, Universiti Malaysia Perlis, Arau 01000, Perlis, Malaysia

[9]Faculty of Civil Engineering Technology, Universiti Malaysia Pahang, 26300 Kuantan, Pahang, Malaysia; ramadhansyah@ump.edu.my

*** Corresponding Authors:** azree@usm.my; alireza.bahrami@hig.se; yozkilic@erbakan.edu.tr

Abstract

Researchers have shown significant interest in the incorporation of nanoscale components into concrete, primarily driven by the unique properties exhibited by these nano elements. A nanoparticle comprises numerous atoms arranged in a cluster ranging from 10 to 100 nanometers in size. The brittleness of foamed concrete (FC) can be effectively mitigated by incorporating nanoparticles, thereby improving its overall properties. The objective of this investigation is to analyze the effects of incorporating calcium carbonate nanoparticles (CCNP) into FC on its mechanical and durability properties. The FC had a 750 kg/m^3 density, which was achieved using a binder-filler ratio of 1:1.5 and a water-to-binder ratio of 0.45. The CCNP material exhibited a purity level of 99.5% and possessed a fixed grain size of 40nm. A total of seven mixes have been prepared, incorporating CCNP in FC mixes at specific weight fractions of 0% (control), 1%, 2%, 3%, 4%, 5%, and 6%. The properties that were

assessed include slump, bulk density, flexural strength, splitting tensile strength, compressive strength, permeable porosity, water absorption, drying shrinkage, softening coefficient, and microstructural characterization. The results suggest that incorporating CCNP into FC enhances its mechanical and durability properties, with the most optimal improvement observed at a CCNP addition of 4%. In comparison to the control specimen, it was observed that specimens containing 4% CCNP demonstrated significantly higher capacities in compressive, splitting tensile, and flexural tests, with increases of 66%, 52%, and 59% respectively. The addition of CCNP resulted in an improvement in the FC porosity and water absorption. However, it also led to a decrease in the workability of the mixtures. Furthermore, the study also provided the correlations between compressive strength and splitting tensile strength, as well as the correlations between compressive strength and flexural strength. In addition, an artificial neural network (ANN) approach was employed, utilizing *k*-fold cross-validation, to predict the compressive strength. The confirmation of property enhancement is verified through the utilization of a Scanning Electron Microscope.

Keywords: Foamed concrete; Calcium carbonate nanoparticles; Mechanical properties; Durability properties; Scanning Electron Microscope

1. Introduction

The expansion of concrete structures in the construction sector is an emerging trend when compared to the progress made in masonry and wood structures [1-8]. Nevertheless, due to the numerous benefits associated with concrete materials, including exceptional strength properties, good flowability, excellent fire resistance, superior thermal and insulation properties, and high impact resistance, it has gained widespread acceptance and utilization in building construction and infrastructure projects worldwide [9-13]. Concrete has been widely utilized due to its numerous advantages, resulting in a significant growth rate of concrete structures in comparison to other types of structures [14-18]. Additionally, frequent improvements are being conducted [19-23]. It has created significant impacts on the expansion and improvement of human civilization during the course of human history [24-26]. Foamed concrete (FC) is widely recognized as a significant material for use in the global construction industry [27-29]. In comparison to traditional construction materials, FC has the potential to offer enhanced performance and cost-effectiveness in multiple applications [30].

FC can be characterized as a lightweight material with a porous or cellular structure, possessing the ability to flow freely. It exhibits versatility and can be effectively utilized in a diverse range of applications [31]. FC may have varying densities, typically falling within the range of 450 to 1950 kg/m^3. Its compressive strength ranges from 1 MPa to 20 MPa [32-35]. However, despite its growing acceptance in the construction industry, FC does have certain drawbacks. These include its high permeability, increased shrinkage, brittle nature, and a greater risk of cracking due to its permeable structure and the presence of voids. These limitations restrict its use in load-bearing applications within building construction, as highlighted by various studies [36-38]. Numerous investigations have suggested that FC may exhibit volatility, particularly in situations where density experiences a decrease. However, even slight variations in FC density can significantly impact the durability of FC. The reduction in FC density resulted in a significant increase in the number of larger-sized voids [39]. Furthermore, it has been observed that at low densities, FC exhibits a high susceptibility to fracture [40]. The utilization of nanoparticles is not a new concept in either the realm of nature or scientific research [41]. The development of new measurement and visualization technologies has led to significant progress in the testing and characterization of nanoscale materials. As a result, nanotechnology has experienced a notable expansion in various industries including polymers, concretes, plastics, electronics, and medicine [42-45]. Various techniques are implemented to enhance the characteristics of supplementary cementitious materials [46].

Nanomaterials represent a relatively recent advancement in the field of material science, with their conceptualization dating back to the early 1980s [47]. The term nanomaterial pertains to materials that possess a thin structure and exhibit particle sizes within the range of 1 to 100nm [48]. These substances are frequently located in the transitional region between atomic masses and macroscopic bodies and encompass a diverse array of powdered materials. Nanomaterials are characterized by their small particle mass and significant specific surface area [49]. The proportion of surface atoms is 20%, which remains consistent even when the fragment size is as small as 20nm. When compared to conventional granular materials, ultrafine powder exhibits a diverse array of exceptional characteristics [50]. Due to their remarkable efficacy, nanomaterials have emerged as a prominent area of investigation within the scientific community and are regarded as a potential catalyst for the next industrial revolution [51]. The favourable performance of ultrafine particles in concrete is largely attributed to the continuous filler of cementitious material composition [52]. Silica fume enhances the strength and durability of cement-based materials due to its smaller granule size and higher activity level [53]. However, both the production and price of the product are relatively affordable. The field

of nanotechnology has led to the development of nanomaterials as a potential substitute for silica fume, addressing the increasing demand for high-performance concrete [54]. Nanomaterials are being increasingly employed in concrete production due to their distinct nano impacts [55].

The utilization of nanoparticles has previously demonstrated a substantial improvement in durability characteristics and mechanical performance [56]. The utilization of appropriate nanoparticles has the potential to enhance both the firmness and properties of the FC simultaneously [57]. The incorporation of nanoparticles into concrete has resulted in enhancements to the material's workability, mechanical properties, durability, and microstructure, as evidenced in the available literature [58]. Various nanomaterials are commonly employed to enhance the structural integrity of conventional concrete. Some notable examples include titanium oxide, carbon nanotubes, silicon dioxide, calcium carbonate, aluminium oxide, limestone, and iron oxide [59]. Due to the notable pozzolanic activity exhibited by Calcium Carbonate Nano Particles (CCNP), they have been successfully utilized as a substitute for traditional silica fume in various cement-based products [60]. CCNP is classified as one of several types of nanomaterials. The formation of Calcium Silicate Hydrate (CSH) gel occurs through the reaction of calcium hydroxide present between the filler and binder. This process enhances the strength property by leveraging the increased activity of CCNP [61]. Recently, there has been a considerable amount of research conducted on the utilization of nano-modified concrete. Numerous studies have revealed that nanoparticles significantly contribute to the enhancement of concrete properties. They can reduce the amount of cement used to a considerable extent and also fill the voids in the materials, thereby enabling them to have a significant influence on enhancing the performance of traditional concrete [62].

In comparison to various other nanoparticles, it has been observed that CCNPs are more cost-effective and can be obtained in significant quantities [63,64]. Prior studies have indicated that the generation of CCNP could potentially be achieved by a plant through the utilization of waste carbon dioxide (CO2). In their study, Batuecas et al. [65] provided a summary indicating that the addition of 2% CCNP results in a reduction of CO2 emissions by approximately 69%. The carbon dioxide (CO_2) emissions of the cement plant have been successfully reduced from 0.96 to 0.30 CO_2 equivalent per kilogram. Therefore, the utilization of CCNP yields two significant outcomes from both economic and environmental standpoints. In a recent study conducted by Poudyal et al. [66], it was discovered that the utilization of CCNP resulted in enhanced early and late-age strengths of concrete. A previous study conducted by the authors presents comprehensive testing results on cement containing different weight

fractions of CCNP [67]. It was determined that a weight fraction of 1% of CCNP yielded optimal outcomes, characterized by enhanced durability and strength properties. In contemporary times, it is crucial to establish a correlation between the mechanical properties of concrete and the mix design through the utilization of diverse methodologies. These relationships offer valuable insights for researchers, academics, and professionals in the industry.

1.1 Research gap

Research has been conducted on the utilization of CCNP in conventional concrete, and the findings indicate that CCNP significantly contributes to the improvement of concrete properties. The application of the CCNP in FC exhibits some limitations, thereby necessitating a comprehensive exploration of their impact on various properties. The existing literature reveals inadequate exploration of the interrelationship between the mechanical and durability properties of CCNP blended FC, hence restricting the comprehension of their interaction.

1.2 Research objectives

Although the effects of nanomaterials on the properties of concrete are well-understood, there has been little research on the impact of nanoparticles on the mechanical and durability properties of FC. The addition of CCNP to concrete has been investigated, but there are still several uncertainties regarding the mechanism by which CCNP may alter the properties of FC. This ambiguity requires clarification. Consequently, this research is an effort to address this need. The objective is to assess the effect of CCNP addition on the mechanical and durability properties of FC. The investigation is expanded to propose a model between mechanical, mechanical, and durability properties.

2. Materials and Methods

Five main ingredients were required for producing the FC specimens in this study. The FC mixes contained ordinary Portland cement (OPC) as the binder, fine aggregate as the filler, clean water, a protein-based foaming agent, and CCNP as an additive.

2.1 Materials

The utilization of CEM-1 class cement, which complies with the specifications outlined in BS-EN 197-1 [68], is suitable for a wide range of applications in the construction industry. These applications include the production of mortars for floor screeds, brickworks, and blockwork joints, as well as the preparation of interior and exterior renders. Table 1 presents the chemical compositions of cement CEM-1 employed in this study, while Table 2 provides a summary of its physical qualities.

Table 1. CEM-1 cement chemical composition

Oxides elements	Percentage (%)
SiO_2	20.87
CaO	62.98
MgO	1.88
SO_3	3.12
Fe_2O_5	3.62
Al_2O_3	4.59
Insoluble residue	1.38
L.O.I	1.56

The properties of the mortar slurry are influenced by both the characteristics of the sand and the composition of the mixture. The gradation curve depicting the fine sand utilized in this experiment is presented in Figure 1. The determination of particle size distribution was conducted using the ASTM C33-03 standard [69]. The density of sand particles used in the study, as stated in ASTM C128-15 [70], was recorded as 2.49 g/cm^3. The sample has a fine grain composition, with 2.69% of the grains falling within the specified size range, with a maximum diameter of 5mm. The given data has a uniformity value of 2.71 and a curvature coefficient of 1.11. Tap water was utilized for mixing, by the specifications provided in BS-EN 3148 [71].

Table 2. CEM-1 cement physical properties.

Properties	Value
Setting time (initial)	101 minutes
Setting time (final)	209 minutes
Consistency	25.1%
Specific gravity	3.13
Specific surface	2422 cm^2/kg

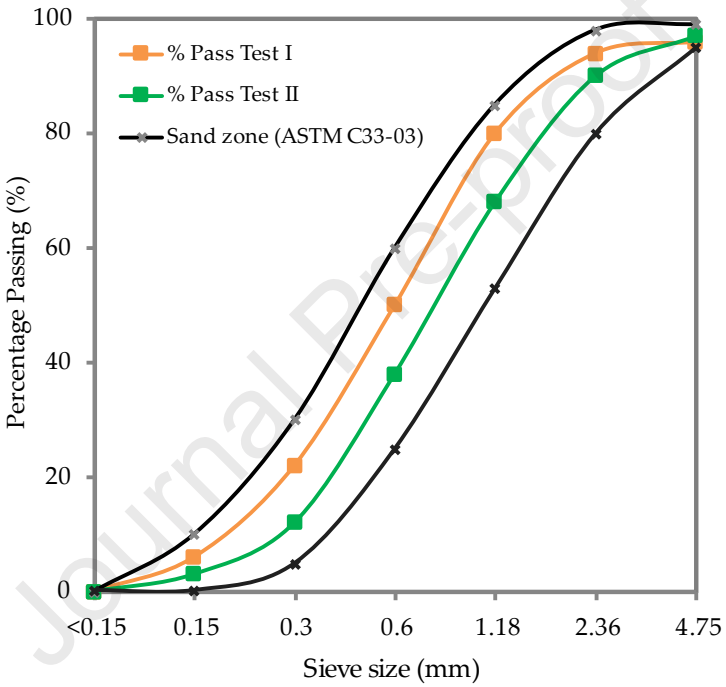

Figure 1. Gradation curve of fine sand

To reduce the apparent friction of a solution and increase the firmness of the foam, a protein foaming agent was used. The properties of the protein foaming agent employed are summarized in Table 3 which was supplied by DRN Technologies Sdn. Bhd., Penang, Malaysia. As protein peptide bonds dissolve, additional hydrophobic molecules are released. When the apparent friction of the solution decreases, an interface is created for air bubbles to form, and the hydrogen bonds between chemical groups aid in the formation of stable bubbles. In comparison to air voids produced using a synthetic foaming agent, the air bubbles formed by this method will be more stable and smaller [72]. The protein foaming agent was applied at a 1:35 ratio with clean water. To achieve a consistent foam, a solution consisting of 1 liter of protein-based foaming agent was mixed with 35 liters of water. A

foam generator was employed. The foam generator has a calibrated foam nozzle with set foam discharge rates ranging from 5 to 15 cubic feet per minute subject to the flow rate

The CCNP utilized in this investigation was obtained from a local supplier, DRN Technologies Sdn Bhd, based in Penang, Malaysia. Tables 4 and 5 present a comprehensive overview of the physical attributes and chemical compositions of CCNP.

Table 3. Properties of foaming agent

Properties	Descriptions/ Values
Type	Protein-based
Product designation	Noraite PA-1
Color	Brown
Foam density (kg/m^3)	75±5
Acidity (pH)	6.45
Specific gravity	1.12
Expansion ratio	14x
Suitable FC density (kg/m^3)	> 700

Table 4. Physical properties of CCNP

Properties	Values
Nanoparticles grain size (nm)	40-60
Purity (%)	99
Density (g/cm^3)	2.89
Colour	White
Molar mass (g/mol)	100.09

Table 5. CCNP chemical composition

Oxides elements	Percentage (%)
CaO	77.29
Fe_2O_3	0.05
SiO_2	0.59
P_2O_5	0.01
Al_2O_3	0.08
SO_3	0.01
K_2O	0.01
MgO	0.14
TiO_2	0.01
Na_2O	0.01
L.O.I	21.8

2.2 Mix design

FC density of 750 kg/m^3 was prepared in this experiment. **Table 6** shows the mix proportion of FC which contain varying weight fractions of CCNP. A binder-filler ratio was maintained at 1:1.5 and the water-binder ratio was set at 0.45. Seven FC mixes in total were produced specifically the control FC (no inclusion of CCNP), CC1, CC2, CC3, CC4, CC5, and CC6 representing varying weight fractions of 1% to 6% addition to FC.

Table 6. FC-CCNP composites mix proportions

FC coding	CCNP (%)	CCNP (kg/m^3)	Binder (kg/m^3)	Filler (kg/m^3)	Water (kg/m^3)	Foam (kg/m^3)
Control	0	0.0	284.4	426.6	128.0	38.5
CC1	1	8.8	284.4	426.6	128.0	38.5
CC2	2	17.5	284.4	426.6	128.0	38.5
CC3	3	26.3	284.4	426.6	128.0	38.5
CC4	4	35.1	284.4	426.6	128.0	38.5
CC5	5	43.9	284.4	426.6	128.0	38.5
CC6	6	52.7	284.4	426.6	128.0	38.5

2.3 Production of FC

The process of producing FC on a small scale is relatively straightforward, requiring neither costly nor complicated machinery. In fact, in many instances, existing equipment used for conventional concrete production can be utilized. In this study, a low-density FC was produced with a constant dry density of 750 kg/m^3 by controlling the foam content added to the cement slurry. There were variations in CC addition specifically 0% (control), 1%, 2%, 3%, 4%, 5%, and 6%. A maximum of 6% weight fraction of CC was selected to avoid FC of reduced density. Firstly, a dry mixture of cement, sand, and CC was mixed for three minutes in a 0.2m^3 capacity tilting concrete mixer. Then, the dry mix was blended with water for an additional three minutes. The production of FC necessitates the presence of an aqueous stable foam, which is considered a crucial component. The foaming generator serves as a medium through which the liquid chemical transforms into a state of stable foam. Therefore, a Portafoam TM-2 machine connected to a premix solution tank (**Figure 2**) was used to generate the

foam as shown in Fig. 1. A premix solution tank-producing system is ideal for use in conjunction with batching equipment. Since just a small amount of foam is needed, it is incredibly cost-effective. Foam liquid concentrates and water is premixed in the tank using pressure tank-producing equipment. The solution is then expelled from the pressure tank through the foam-producing nozzle. The procedure is done only by air pressure. The pressure tanks had a capacity of 40 liters. While calibrated foam nozzles for the pressure tank system are available. This foam generator will also automatically combine liquid foam concentrate with water and compressed air in predetermined quantities. It will suction liquid foam concentrate constantly from the concentrate's container. The liquid foam concentrate is metered and blended with water to make a premixed solution with the appropriate concentration ratio to achieve the required FC density. An air compressor is then used to pressurize and balance the solution. This compressor's air and the premixed solution are then metered via a nozzle, the output of which is controlled by the foam generator. The nozzle is intended to produce a fine micro-bubbled foam of a certain density and quantity. To measure its density, a 5-liter container was used and the density of the foam should be between 70-80 kg/m^3. Once the density was confirmed to be within the acceptable range, it had been inserted into the mortar slurry mix and the mixer was run for a few more minutes until there was no noticeable foam left in the drum. According to ASTM C 1437 [73], a flow table test was conducted to determine the consistency of newly mixed FC. Then, the homogenous FC mix was placed in steel moulds. A plastic sheet was placed over the moulds for 24 hours to protect them from moisture. The samples were cured by moisture curing as soon as they had been demoulded until they were ready for testing.

Figure 2. A Portafoam TM-2 machine was utilized to produce the stable foam

2.3 Experimental procedure

Various tests were conducted to evaluate the mechanical and physical properties of FC, including flexural strength, compression strength, splitting tensile strength, porosity, slump flow rate, and water absorption. A prism with dimensions of 100 x 100 x 500mm was utilized to execute the flexural test, following the guidelines outlined in the BS-EN 12390-5 standard [74]. The compression test was conducted using FC cubes measuring 100 x 100 x 100mm, by the specifications outlined in the BS-EN 12390-3 [75] standard. Subsequently, a cylindrical specimen with a diameter of 100mm and a height of 200mm was employed to determine the splitting tensile strength. The splitting tensile test conducted adheres to the guidelines specified in the BS-EN 12390-6 [76] standard.

The investigation also encompassed an assessment of the water absorption and porosity properties of FC. The softening coefficient is a significant indicator used to characterize FC. The softening coefficient pertains to the capacity of a specific FC mixture to withstand water damage, and it exerts a notable impact on materials characterized by elevated levels of water absorption and porosity. The softening coefficient was determined based on the high water absorption and porosity of FC. It was calculated as the ratio of the compressive strength of FC when saturated with water to its compressive strength in a dry condition.

Furthermore, the porosity of FC was assessed using a vacuum saturation technique [77], and a water absorption test was accomplished by the BS-EN 1881-122 standard [78]. In accordance with the ASTM C878/C878M-22 standard [79], a drying shrinkage test was conducted to determine the volumetric contraction of FC due to moisture loss. This test involved the use of a prism measuring 75mm x 75mm x 290mm. Besides, the workability test was also achieved in agreement with the standards established by ASTM C 230-97 [80].

3. Results and Discussion

3.1 Slump

Slump flow must be taken into account when evaluating FC performance. The workability of FC-CCNP composites in relation to slump value is depicted in Figure 3. As seen in Figure 3, the slump flow of FC blends decreased as CCNP content increased. The control FC achieved the greatest slump flow diameter, measuring 259mm, while FC with a 6% CCNP recorded the smallest slump flow diameter, measuring 238mm. The results are consistent with those of Supit and Shaikh [81]. Compared to the control FC, the slump flow of the FC containing CCNP is reduced. As the weight fraction of

CCNP in the mixture increases, the fluidity decreases. The workability of the FC containing 1% CCNP is lower than that of the control FC. The decrease in the workability of FC is due to the CCNP's higher specific surface area. Meng et al. [82] found that water usage increases along with the CCNP weight fraction. The water demand experiences a modest rise of 0.4%, 1.8%, and 3.2% correspondingly, reliant upon the CCNP weight fraction being 1%, 3%, or 5%. However, this influence is lessened when a CCNP intermediate slurry is employed. With the addition of CCNP from 1% to 6%, slump flow falls by 1.2%, 3.9%, 5.0%, 5.4%, 6.9%, and 8.1% in comparison to the control FC. The CCNP medium slurry is faster to dissipate uniformly and may greatly improve particle size dispersion, which is the main justification for this modification. The presence of CCNP could accelerate setting time in addition to enhancing cement hydration.

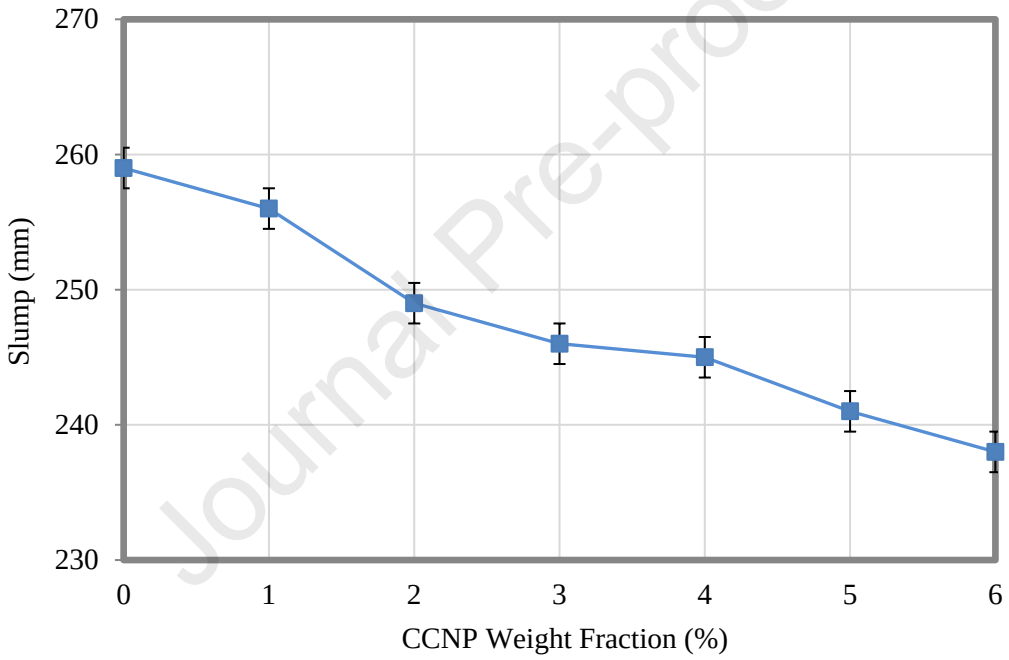

Figure 3. The slump of FC-CCNP composites

3.2 Density

The material's varying densities are influenced by a combination of several factors, including the inclusion of different types of cement, sand, foaming agent, and the incorporation of an additive in the FC base mix. However, maintaining FC densities within a range of roughly ± 60 kg/m^3 of their targeted final density is of utmost significance. Figure 4 illustrates the relationship between the influence of varying weight fractions of CCNP on the FC densities. The observed trend in Figure 4 indicates that there is a slight increase in FC density as the weight fraction of CCNP increases (from 1% to 6%) and

as the curing age progresses from day 7 to day 56. On the 28th day, the FC mixture, which consisted of a 6% weight percentage of CCNP, exhibited a density of 770 kg/m^3. In contrast, the control FC displayed a density of 755 kg/m^3. The FC specimen, containing a 2% CCNF, exhibited a density of 756 kg/m^3 after 7 days of curing. Subsequently, the density increased to 759 kg/m^3 on day 28 and further rose to 764 kg/m^3 on day 28 of the curing process. On the 56th day, however, the density remained satisfactory. On day 28, control, CC1, CC2, CC3, CC4, CC5, and CC6 exhibited variations in density compared to the target values of 9, 12, 14, 16, 17, 18, and 22 kg/m^3. The density increase was attributed to the higher specific gravity of CCNP within the FC cementitious matrix [83]. Furthermore, the incorporation of CCNP into FC has the potential to improve the density of grain filling, reduce the fraction of voids in solid fragments, and enhance the availability of free water for lubricating [84]. The plastic viscosity may increase as a consequence of these opposing mechanisms. Furthermore, the incorporation of CCNP into FC has been observed to result in a rise in water consumption, as well as higher yield stress and viscosity [85]. The CCNP is utilized as a filler material in the FC matrix, resulting in a decrease in porosity and voids, hence enhancing the density of the FC [86].

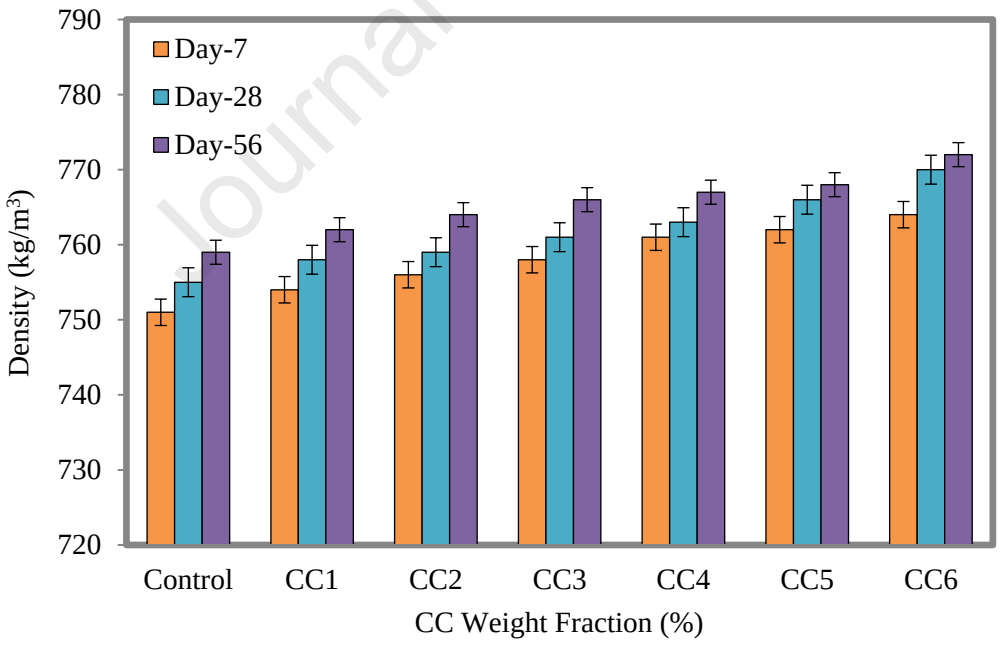

Figure 4. The density of FC-CCNP composites

3.3 Flexural strength

Figure 5 illustrates the influence of the incorporation of different weight fractions of CCNP on the flexural strength of FC. The results indicate an initial rise of up to 4% in flexural strength with the addition of CCNP. However, as the CCNP content further increases, the flexural strength gradually declines. At the age of 28 days, the addition of CCNP at weight fractions of 1%, 2%, 3%, 4%, 5%, and 6% resulted in increases in flexural strength of 7.46%, 22.39%, 30.26%, 58.75%, 23.57%, and 2.31%, respectively. The CC4 blend exhibits a substantially greater increase in flexural strength compared to the other mixes. An observed increase in flexural strength is recorded for the CC4 mix, with a rate of 18.75% at 28 days and 34.38% at 56 days compared to the 7th day. The observed increase in flexural strength can be attributed to the ability of the matrix material to transmit loads to the CCNP. The CCNPs exhibit a strong bonding with the cement matrix because of their superlattice nature, characterized by enhanced van der Waals forces at the contact. Moreover, the CCNP induces the formation of a compact arrangement of hydration products, resulting in a wider range of particle sizes and a decrease in the dimensions and connectivity of pores, hence improving flexural strength. The packing density of a matrix is enhanced when CCNP is incorporated into an FC cementitious matrix, resulting in strengthened bonding between the filler and binder at the interfacial transition area. Moreover, the presence of non-uniformly distributed particles, caused by a critical concentration of more than 5% of the CCNP in FC, may have contributed to the decline in flexural strength [87]. The literature suggests two possibilities for the observed rise in flexural strength. Firstly, it implies that the presence of CCNP fills the micropores within the cementitious matrix, leading to an increase in density. Secondly, the production of new hydrated components is proposed as an additional factor contributing to the enhanced flexural strength [88]. The incorporation of CCNP at its minimum concentration leads to a notable enhancement in flexural strength. Liu et al. (89) specifically documented that the inclusion of 1% of CCNP resulted in a significant enhancement in flexural strength as compared to the control sample. A decrease in flexural strength was seen at greater replacement levels, which can be attributed to inadequate dispersion and agglomeration of nanoparticles within the cementitious composites [90].

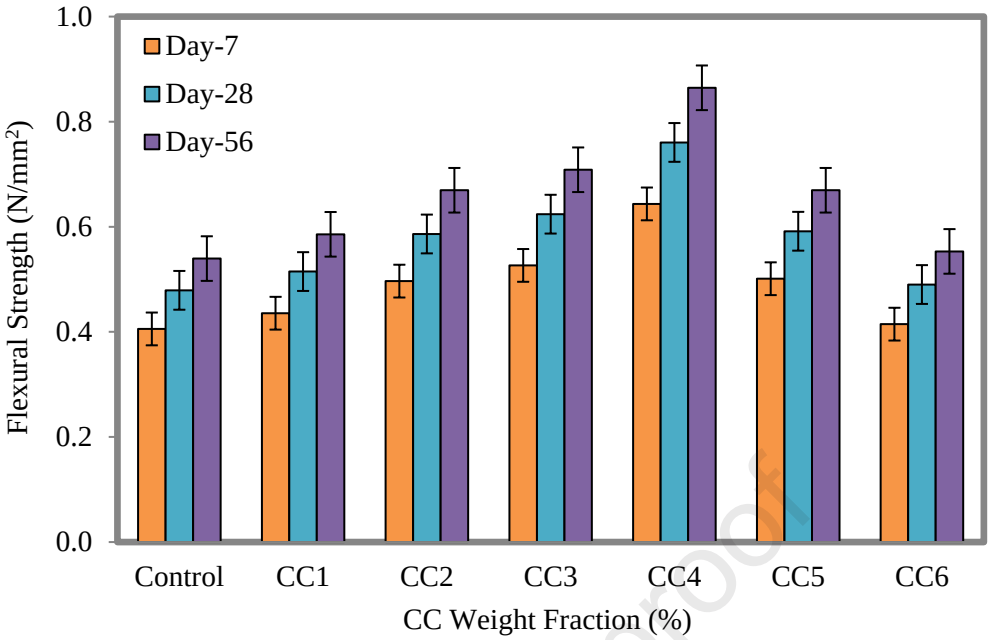

Figure 5. Flexural strength of FC-CCNP composites

3.4 Splitting tensile strength

In line with the findings on flexural strength, it was observed that an increase in the weight fraction of CCNP resulted in an enhancement of the splitting tensile strength of FC at 7, 28, and 56 days, as illustrated in Figure 6. The splitting tensile strength of the samples increased by 7%, 21%, 24%, and 52% at 28 days, and by 8%, 24%, 32%, and 52% at 7 days, respectively. These improvements were observed when weight fractions of 1%, 2%, 3%, and 4% of CCNP were added to the samples, as compared to the control sample. However, following the incorporation of a 4% CCNP, there was a gradual decrease observed in the splitting tensile strength. The CCNP is known for its intricate nature, characterized by its nanoscopic scale, significant interfacial area, and precise atom arrangement. When exposed to external stress, the atoms exhibit rapid migration, absorb energy during this process, and demonstrate resistance to deformation. When force is exerted on the FC, it results in the formation of an internal network of microcracks, ultimately leading to the fracture of the FC. This fracture is portrayed by the presence of numerous small and major cracks. The emergence, growth, and coalescence of internal fractures have a detrimental effect on the load-bearing surface of the FC matrix. The reduction in the effective load-bearing area also leads to an increase in the stresses at major fracture points. The presence of CCNP enhances fracture resistance and mitigates crack propagation. The

CCNP possesses a significant aspect ratio and shape that enables it to effectively obstruct and redirect microcracks, thereby exhibiting robust properties for inhibiting crack advancement [91]. Additionally, the bridging function of CCNP particles can effectively prevent and mitigate the propagation of fractures. Certain fractures tend to naturally close when subjected to compressive pressure, however, the occurrence of crack merging becomes more prominent when exposed to tensile strain [92]. Although the addition of CCNP into FC beyond 4% exhibits a decreasing trend, it is noteworthy that the splitting tensile strength at weight fractions of 5% and 6% of CCNP is still 17% and 7% higher, respectively, compared to the control FC on day 28.

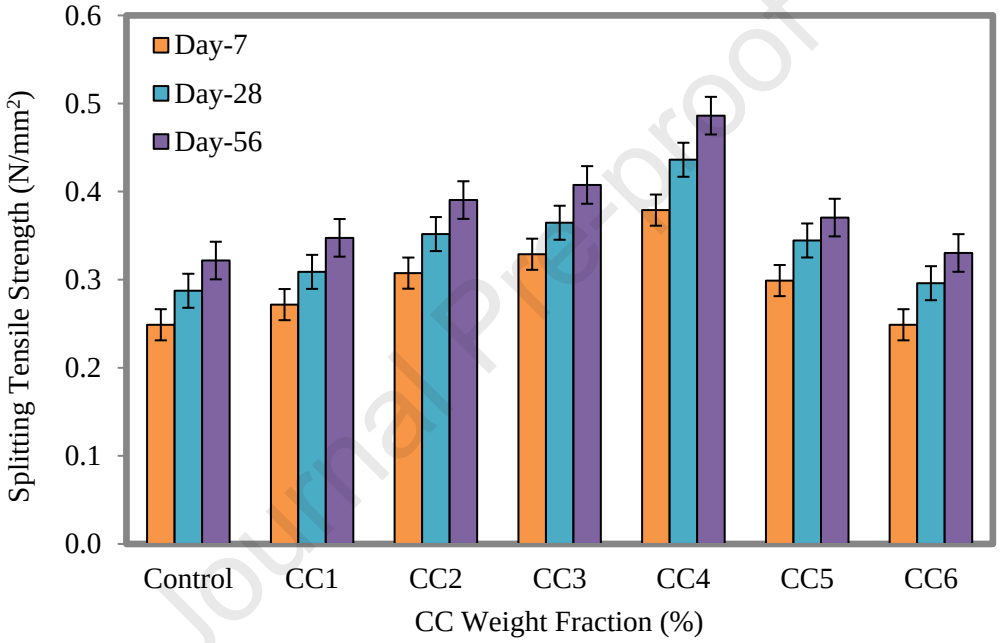

Figure 6. Splitting tensile strength of FC-CCNP composites

3.5 Compressive strength

According to Figure 7, there is a positive correlation between the weight percentage of CCNP and the compressive strength of FC. The compressive strength of FC increases as the weight fraction of CCNP increases, with the highest value observed at an optimal weight fraction of 4%. A 6% CCNP experienced an increase of 14.3%. The inclusion of a 4% weight fraction of CCNP resulted in a notable enhancement of the compressive strength, reaching 3.36 MPa. This improvement represents a significant 66% increase compared to the control FC. Within the FC cementitious matrix, these elements collaborate synergistically to enhance compressive strength. The inclusion of a 5% concentration of CCNP resulted in a 15% increase in compressive strength compared to the control sample. This improvement is lower than the increase observed with the addition of 3% CCNP.

Nanoparticles with high specific areas are vulnerable to clustering due to secondary interactions [93]. There is an observed increase in the compressive strength of the specimens when CCNP is added at different weight fractions. Specifically, there is an increase of approximately 12.78%, 26.52%, 32.27%, 65.18%, 14.38%, and 3.19% when CCNP is added at 1%, 2%, 3%, 4%, 5%, and 6% respectively, compared to the control specimen FC. These results were obtained after conducting a 28-day testing of the FC specimens. Additionally, it is observed that the compressive strength rate increases for a duration of 28 days when compared to a duration of 7 days. The inclusion of CCNP in the FC leads to the production of minerals such as calcium silicate hydrate (C-S-H) and calcium aluminate silicate hydrate (C-A-S-H), which play a significant role in enhancing mechanical properties. In addition, CCNP is utilized as a filler material to enhance density and subsequently improve strength properties. The increase in compressive strength can be attributed to the accelerated reaction rate of tricalcium aluminate, resulting in the production of a greater amount of carbon aluminate complex. Consequently, this leads to an increase in the hydration compounds [94]. Furthermore, the nanoparticles of CCNP exhibit a reactive behavior when interacting with tricalcium silicate, resulting in an enhanced rate of hardening and development of FC. This effect is particularly noticeable when the replacement level is lower and during the early stages of FC strength. The reaction of tricalcium aluminate and tricalcium silicate with CCNP leads to the formation of a significant quantity of hydration products. These products consume the available water, effectively counteracting the dilution effect of the bonded materials. Consequently, this process contributes to an enhancement in strength. The inadequate dispersion of CCNP particles and the presence of van der Waals forces in the binder can be identified as factors contributing to the achievement of an optimized level of CCNP.

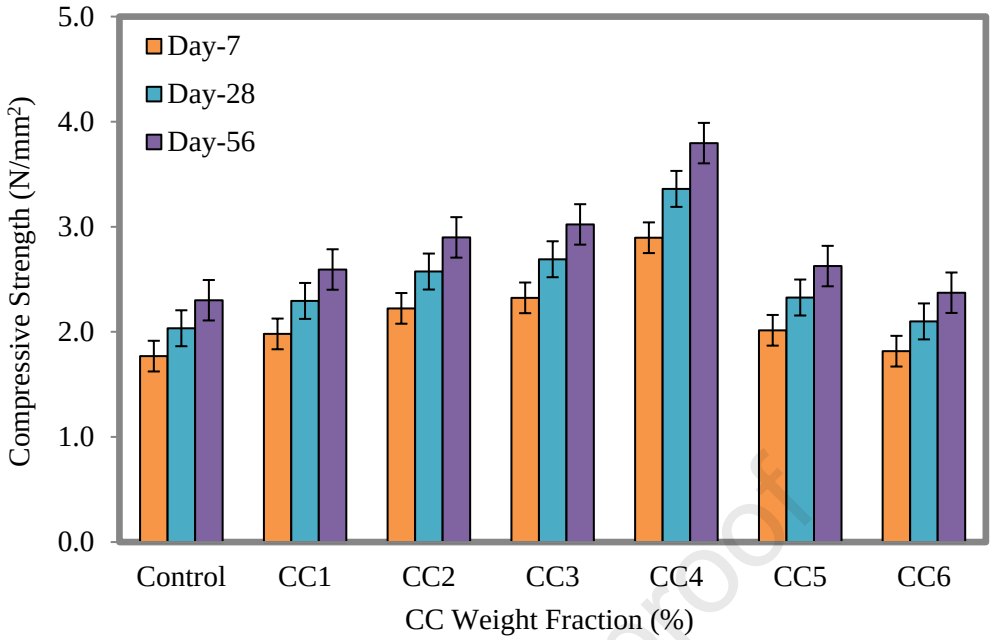

Figure 7. Compressive strength of FC-CCNP composites

3.6 Porosity

The results of the permeable porosity of FC-CCNP composites are depicted in Figure 8. The increase in the weight percentage of CCNP in the FC mixes resulted in a decrease in permeable porosity. The inclusion of 3% and 4% of CCNP in the control FC results in an enhancement of permeability porosity by 6% and 9% correspondingly, when compared to the control FC. The introduction of CCNP into the pores at the interface between the binder paste and the filler resulted in a decrease in the activity of capillary pores. It is important to note that the pores were filled with CCNP. The observed trend in permeability porosity values can be attributed to the alteration of the microstructure in the presence of CCNP. These CCNP hold together to form a gel chain by acting as kernels, and this is one of the reasons why such a trend can be observed in the permeable porosity values [95]. The CCNP is employed to address the discrete and continuous gaps observed in the specimens, resulting in a reduction of capillary suction that facilitates water absorption into the FC specimens. The observed effect involves a reduction in the size of the biggest pores on the outer surface as a result of the production of newly hydrated compounds, which is attributed to the increase in the content of CCNP. As previously mentioned, it has been shown that CCNP exhibits involvement in the hydration reaction, hence facilitating the hydration process of various cementitious materials. Additionally, CCNP effectively occupies voids within the cement matrix, resulting in a reduction of pore volume [96].

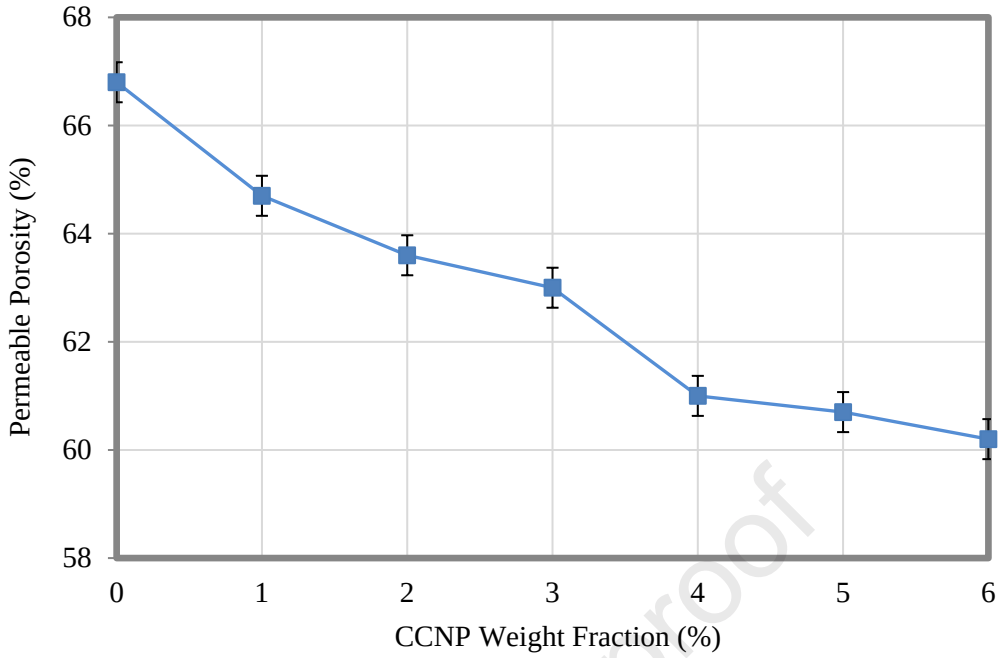

Figure 8. Permeable porosity of FC-CCNP composites

3.7 Water absorption

Figure 9 shows the outcomes of the water absorption of FC-CCNP composites. It appears that water absorption gradually decreases as CCNP content increases. The control FC's water absorption value was 25.8%. A 6% weight fraction of CCNP in FC demonstrates a significant decrease in water penetration when compared to all other weight fractions of CCNP. This is so that the FC mixture's gel pores can be sealed off owing to the lower particle size. With the addition of a 6% CCNP, the water absorption capacity was determined to be 22.9%, which is a decrease of nearly 11% from the control specimen. The reason is due to the densified microstructure and refined pores. With a 4% addition of CCNP, a significant decrease in water absorption from the control sample to FC-CCNP composites is apparent. This effect also occurs with greater weight fractions of CCNF in FC. Above the 4% weight fraction of CCNP in FC, the decrease in water absorption capacity is minimal. An increase in CCNP causes a decrease in water absorption because it increases the hydration products, absorbs more calcium hydroxide, and causes the formation of new gels to fill the matrix's gaps, decreasing the porosity of FC [97].

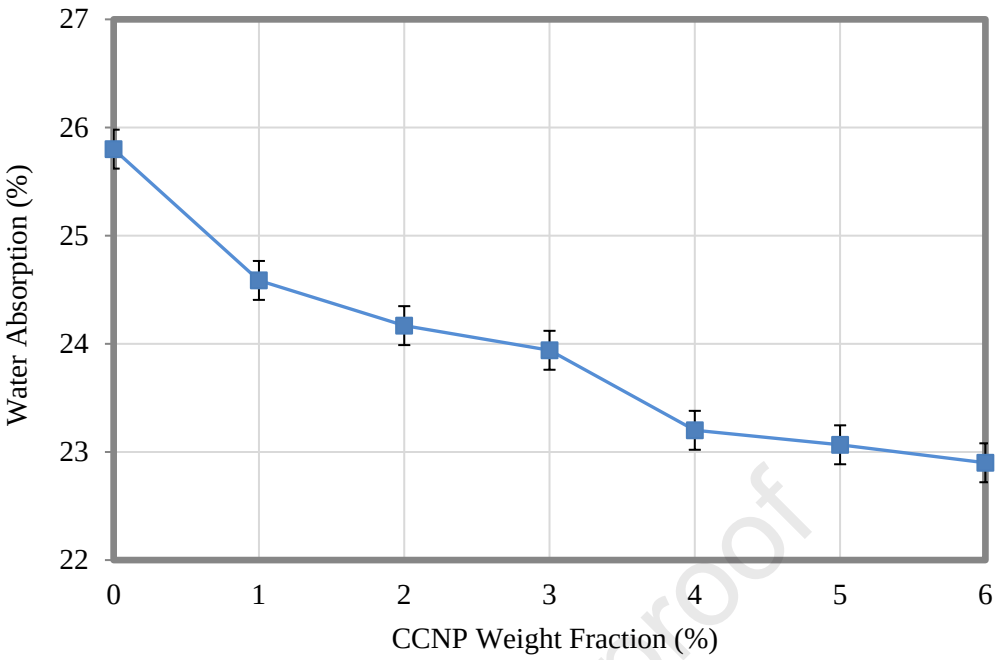

Figure 9. Water absorption of FC-CCNP composites

3.8 Drying shrinkage

The drying shrinkage of FC is a phenomenon characterized by a decrease in volume primarily due to the evaporation of water from the FC in conditions of low ambient humidity. This particular type of shrinkage is widely recognized as a leading cause of concrete cracking. The cement paste used in FC is considered to exhibit viscoelastic behavior, meaning that its volume change is influenced by both elastic and viscous mechanisms. The results of drying shrinkage of FC-CCNP composites are illustrated in Figure 10. As depicted in Figure 10, the drying shrinkage exhibited an increase over time for all mixtures. Overall, it was observed that the control mix exhibited the greatest degree of drying shrinkage. The incorporation of CCNP in FC results in a substantial reduction in drying shrinkage. The presence of 4% CCNP in the FC mix (mix CC4) led to the attainment of the optimal outcome. The CCNP exhibits the ability to absorb tensile energy while the FC material undergoes shrinkage. This energy transfer occurs at the interface between the CCNP and FC matrices, resulting in the dispersion of energy to the adjacent matrix. Consequently, the concentration of tensile stress within the FC matrix decreases, thereby enhancing its resistance to crack propagation. According to Abellan-Garcia et al. [98], when the weight fraction of CCNP in the FC matrix exceeds 4%, inadequate dispersion of CCNP within the FC matrix results in the agglomeration of nanoparticles. Consequently, this phenomenon

impedes the ability of CCNP to effectively disperse tensile stress from the FC region to other areas via its surface. This explanation provides support for the assertion that there is no substantial enhancement in the resistance to drying shrinkage cracking beyond a weight fraction of 4%. When a suitable weight proportion of CCNP is uniformly distributed within the cement paste composed of FC, the resulting hydrated cement products tend to accumulate around the CCNP. This phenomenon can be attributed to the higher surface energy of the CCNP, which serves as a favorable site for nucleation.

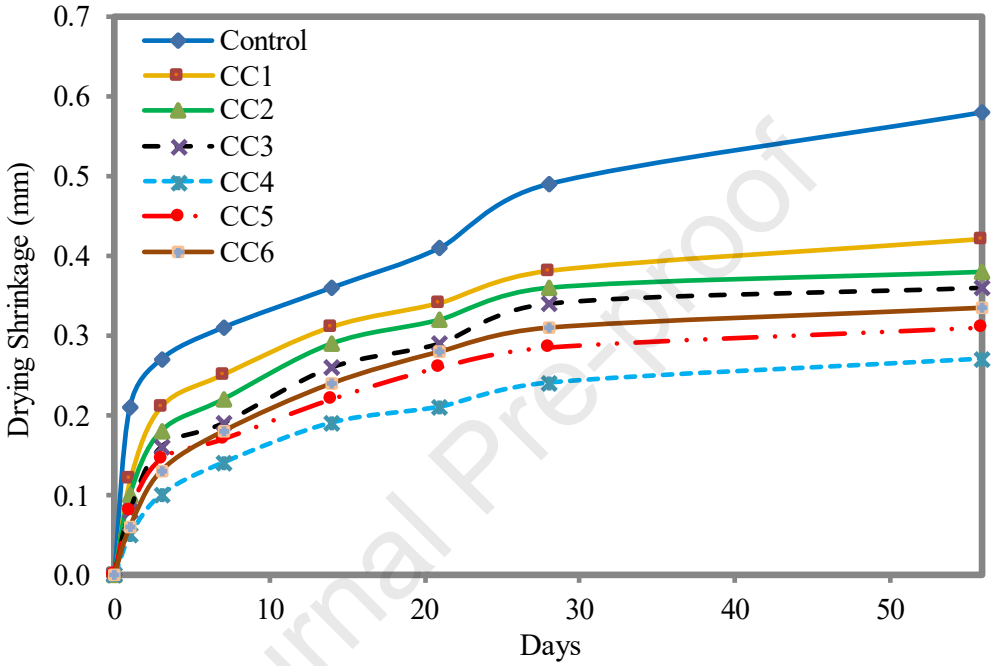

Figure 10. Drying shrinkage of FC-CCNP composites

3.9 Softening coefficient

If FC-CCNP composites undergo water absorption and possess inadequate water resistance, it will significantly hinder the expected lifespan of the FC as an insulation material. The softening coefficient is a substantial consideration that distinguishes the water resistance properties of cement-based materials. It is expressed as the proportion of the compressive strength exhibited by FC when saturated with water to the compressive strength of FC observed when it is in a dry state. **Figure 11** shows the softening coefficient of FC-CCNP composites. The data presented in **Figure 11** illustrates that the softening coefficient is consistently below 1.00 across all FC-CCNP mixtures. This indicates that the presence of water saturation has a detrimental impact on the compressive strength of FC-CCNP composites. The experimental results demonstrate an upward trend between the weight fraction of

CCNP and the softening coefficient of FC-CCNP composites, up to a weight fraction of 4% (referred to as mix CC4). The mix CC4 displayed the highest softening coefficient of 0.94, in contrast to the control mix which had the lowest softening coefficient of 0.85. For CC5 and CC6 mixes, the softening coefficient decreased slightly to 0.91 and 0.90, respectively, when exceeding 4%. In general, it is recommended that the softening coefficient of water-resistant materials, such as FC, should be more than 0.85 [99]. Hence, based on the softening coefficient obtained in this research, it is justifiable to assert that all FC-CCNP blends examined in this investigation exhibit a good level of water resistance capability. The relationship between the water resistance of a material and its pore structure and particle adhesion method is widely acknowledged in the literature [100]. Hence, the reduction of porosity in FC is a crucial method for enhancing its mechanical properties.

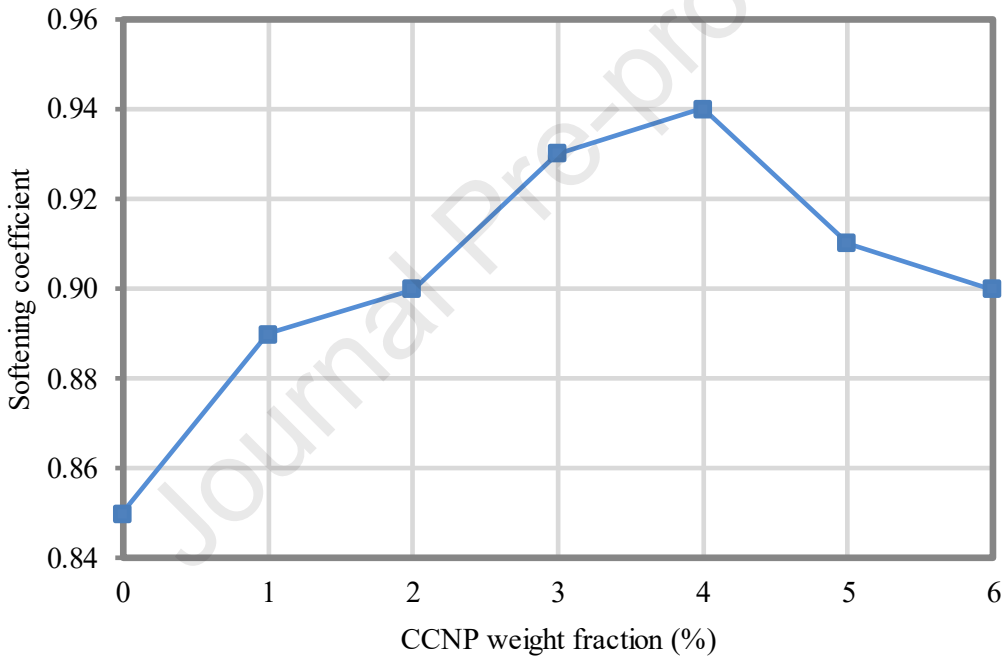

Figure 11. Softening coefficient of FC-CCNP composites

3.10 Microstructural study

Figure 12 displays the scanning electron microscope (SEM) images of the control FC in comparison to the FC containing various weight fractions of CCNP. The control FC (as shown in Figure 12a) exhibits greater void sizes and connected pores. The inclusion of CCNP in the composition of the base mixture resulted in a significant reduction in void sizes, as depicted in Figures 12b-f. In addition to the aforementioned point, the presence of the CCNP leads to an increase in the density of

the matrix as a result of enhanced development of the C-S-H (Calcium Silicate Hydrate). This occurrence is confirmed by observed enhancements in both density and strength properties. The strength of FC was augmented by the widespread dispersion of C-S-H gel within the cementitious matrix that had been hydrated with FC. The presence of Ca(OH)2 and CaCO3 was found on the external surface of the hydrated FC cement paste. The strength of the mixture was notably increased as a result of the expansion and dispersion of mineral elements. The control FC exhibits a pore diameter of 0.69mm. However, upon the introduction of 1% of CCNP, the pore size decreases to 0.66mm, suggesting the presence of newly formed hydration compounds. Furthermore, with the inclusion of CCNP, the void size was decreased to 0.53mm for the CCN3 mixture. Additionally, for the 3% concentration of CCNP, the void size was further reduced to 0.39mm. This suggests that an increase in the incorporation of CCNP leads to a greater generation of hydration products. Additionally, the inclusion of CCNP results in the filling of pores, thereby raising the density of the mixture. The CCN4 mix has an optimal mix proportion, characterized by a void size of 0.26mm, which suggests a higher concentration of hydration products and pore filling. This leads to an increase in density. In a study conducted by Martinez-Garcia et al. (2021) [101], it was shown that the production of hydrated products led to a reduction in void size, which was consistent with previous findings. The introduction of new products also contributed to this effect. In addition to a 4% increase in the content of CCNP, a layer composed of hydrated cementitious materials, specifically Portlandite and Calcite, was placed on top of the compacted cement matrix. The lack of calcium in the combination may have hindered the breakdown of C-S-H. The decreased strength of mix CCNP5 can be ascribed to insufficient mineral element development inside the composite. The decreased indication and dispersion of C-S-H can be attributed to the presence of unreacted particles in the supplementary substance. The C-S-H gel experienced a significant breakdown, leading to the formation of calcite crystals. The diminished strength of CCNP5 was noted as a result of the existing microstructural circumstances. In addition, it was observed that the composite had inadequate mechanical properties, and the chemical interaction between Portlandite and Silica content ceased after a period of 28 days.

According to the observations made in Figure 12, it can be noticed that the equidimensional spherical nanoparticles were accompanied by rhombohedral crystals at the nanoscale. The production of calcite has been reported by Jagadesh et al. [102]. The reaction between the tri-calcium aluminate and the gypsum results in calcium sulfoaluminates or ettringite and thereby the reduction of the gypsum. The conversion of calcium sulfoaluminates to monosulfoaluminates was necessitated by the unavailability of gypsum. The transformation of monosulfoaluminates is modified with the

incorporation of CCNP. The carbonates present in the CCNP cement experience a chemical reaction with tri-calcium aluminate in the FC, resulting in the formation of calcium carbon-aluminates. The inclusion of CCNP results in the substitution of sulphate ions in calcium sulfoaluminates and monosulfoaluminates with carbonate ions, hence enhancing the stability of calcium sulfoaluminates [103]. Based on the observations made in Figure 12(e), it can be inferred that a condensed arrangement characterized by a reduced presence of hydration products within the C-S-H gel, along with a lower occurrence of sulfoaluminates, leads to the development of a more tightly packed structure. Consequently, this denser matrix exhibits an enhancement in its mechanical capabilities. Based on microscopic observations, it can be inferred that the formation of a denser matrix can be attributed to the existence of small C-S-H gel products and the filling of spaces by nanoparticles, thereby leading to an increase in density.

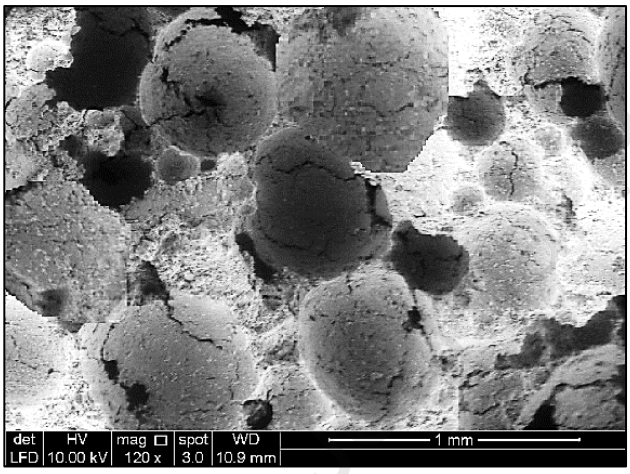

(a) CC0

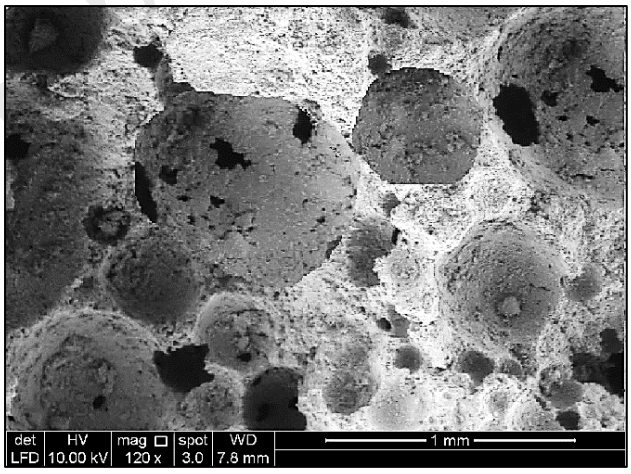

(b) CC1

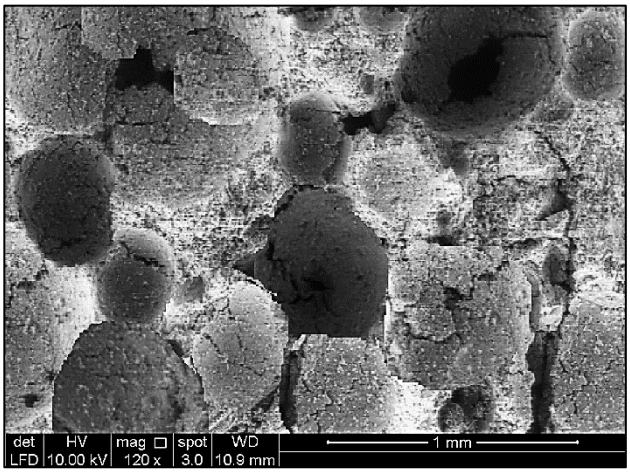

(c) CC2

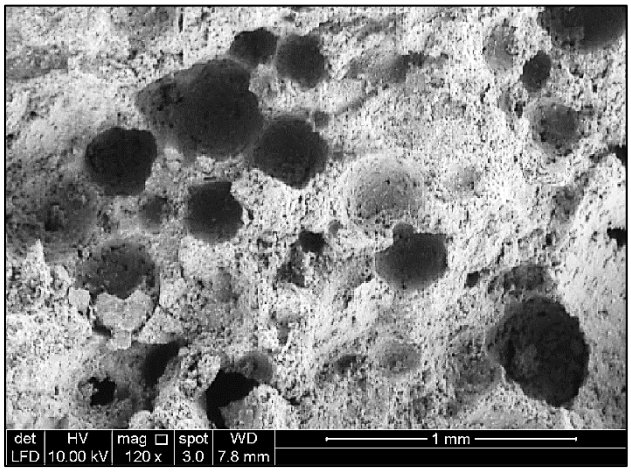

(d) CC3

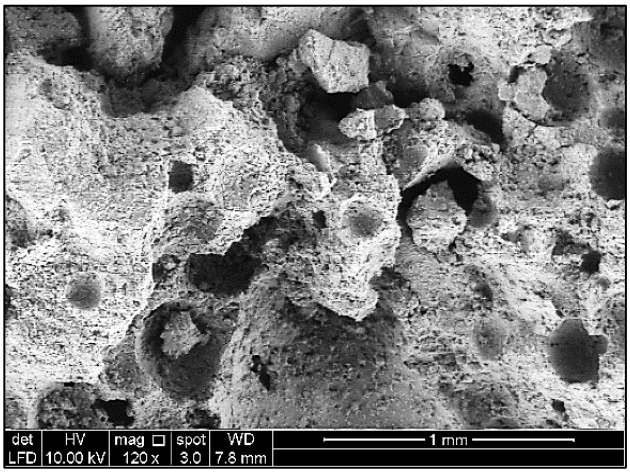

(e) CC4

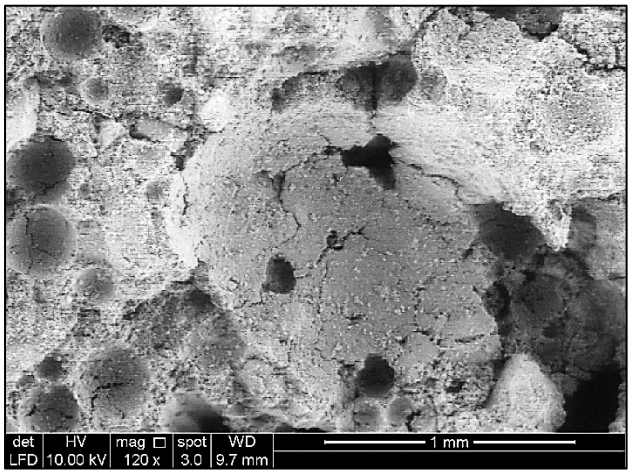

(f) CC5

Figure 12. SEM micrographs (a) control FC; (b) FC with the inclusion of 4% CCNP

4. Correlation analysis between FC-CCNP properties

To accurately determine the properties of FC, it is necessary to obtain information regarding its other properties or the constituents materials used in the mixture. These correlations are necessary for cost savings, environmental resource conservation, manpower efficiency, time efficiency, and other benefits for researchers, academics, and professionals in the industry. Martinez-Garcia et al. [104] reported on the influence of various factors on the strength properties of concrete. Therefore, it is imperative to quantify one of the mechanical properties of FC-CCNP by estimating it from other mechanical properties. Correlation expressions have been developed to establish the relationship between the properties of FC-CCNP. The fundamental linear correlation method was employed to investigate the relationship between physical properties and strength properties. Figure 13 displays the correlation analysis conducted on the compressive and flexural strengths of FC-CCNP composites. The power relations among all FC-CCNP specimens exhibited a strong correlation. The compressive and splitting tensile strengths exhibit a strong positive linear relationship, as evidenced by an R-squared of 0.998. In the majority of literature pertaining to the relationship between compressive strength and flexural strength, it is observed that a power relationship exists between these two strengths.

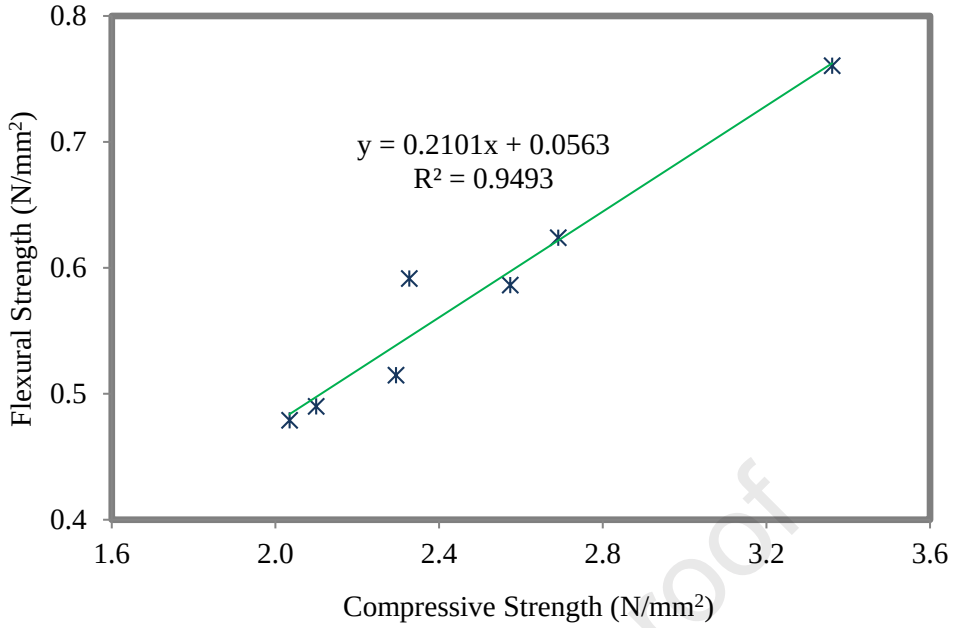

Figure 13. FC-CCNP composite compressive-flexural strengths correlation analysis

The relationship between the compressive and splitting tensile strengths of FC-CCNP composites is illustrated in Figure 14. The data distribution depicted in Figure 14, with an R-squared value of 0.995, provides evidence supporting the assertion of a significant relationship between the compressive and split tensile strength of FC reinforced by CCNP. By the existing literature, there exists a correlation between compressive strength and split tensile strength, which can be described as a power relationship. Figure 15 provides evidence supporting the correlation between the flexural and splitting tensile strengths of FC. Based on the R-squared value of 0.997, it is evident that a strong linear correlation exists between the two strength parameters.

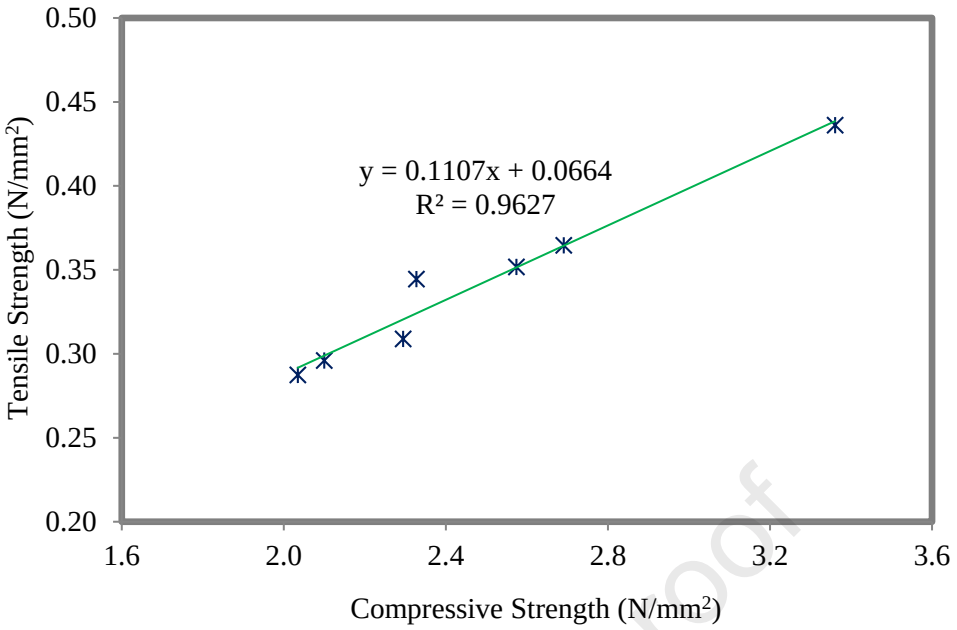

Figure 14. FC-CCNP composite compressive-tensile strengths correlation analysis

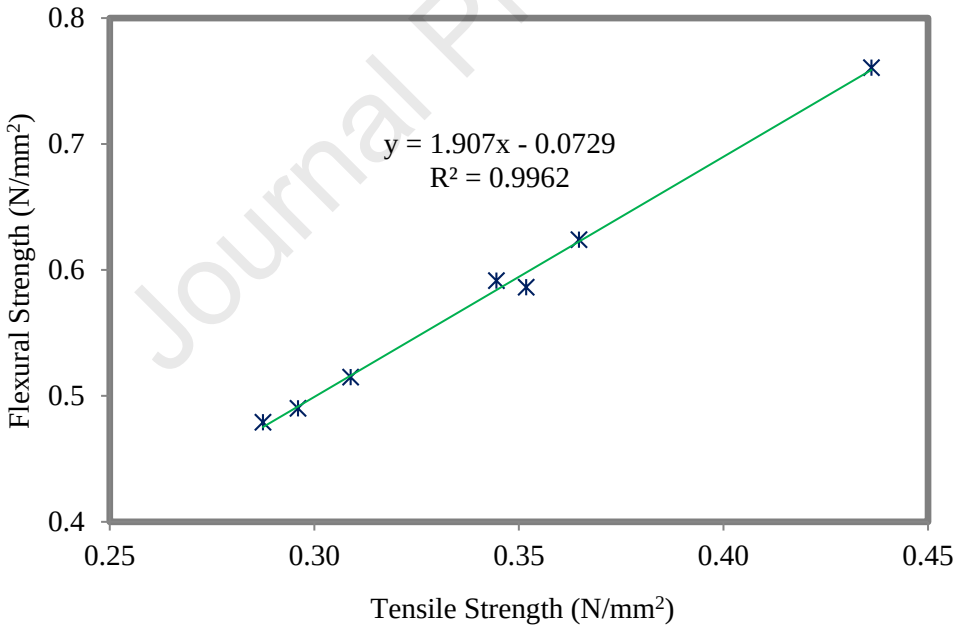

Figure 15. FC-CCNP composite flexural–splitting tensile strengths correlation analysis

Additionally, Figure 16 illustrates the correlation between permeable porosity and water absorption of FC-CCNP composites. An R-squared value of 0.9881 was achieved. The correlation indicates that there is a positive relationship between porosity and water absorption value, whereby an increase in porosity leads to an increase in water absorption. The correlation expressions presented

indicate a significant relationship between changes in the variables and corresponding changes in the response variable. Furthermore, the prediction models developed demonstrate a substantial level of explanatory power, accounting for a significant proportion of the observed variability. It is important to note that the correlation expressions suggested in this study can be utilized in the design of nanoparticle-modified FC.

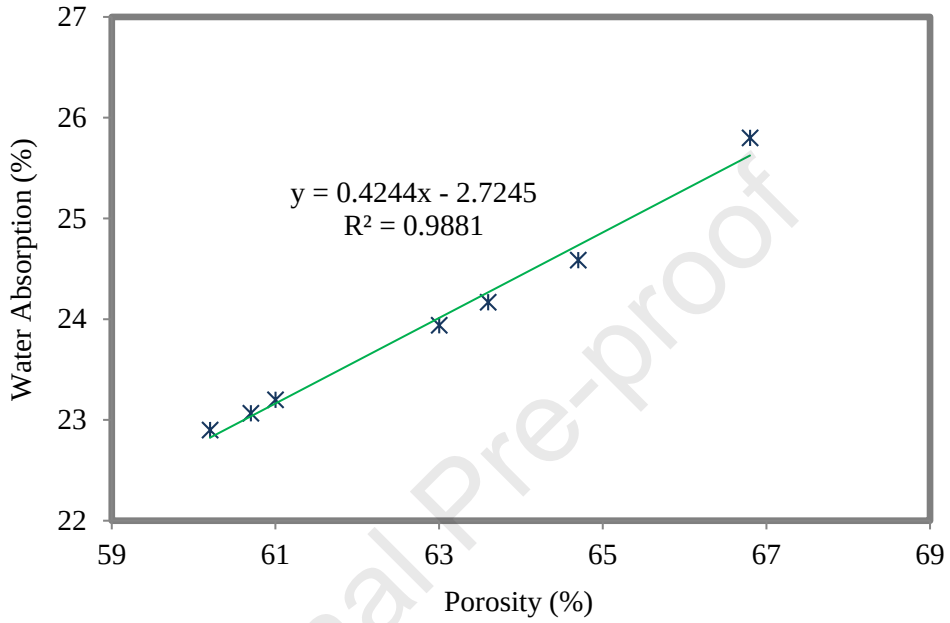

Figure 16. FC-CCNP composite porosity-water absorption correlation analysis

5. Compressive Strength Estimation using Artificial Neural Network

Artificial Neural Network (ANN) is a machine learning model that exhibits similarities to the neural networks present in the human brain. Artificial neural networks (ANNs) have been extensively utilized in various engineering applications due to their capability to effectively model intricate nonlinear systems [105]. One application chosen for analysis in this study involves the estimation of the compressive strength of FC. To achieve an optimal blend and attain the desired level of strength, significant financial, temporal, and human resources are required, along with the consumption of natural resources. The ANN technique is utilized, employing the feedforward propagation method, to estimate the compressive strength of FC during a specified testing period. The compressive strength can be determined by employing a neural network architecture with the number of hidden layers set equal to the number of input variables. According to Figure 17, the number of layers employed for the modeling process using ANN is depicted.

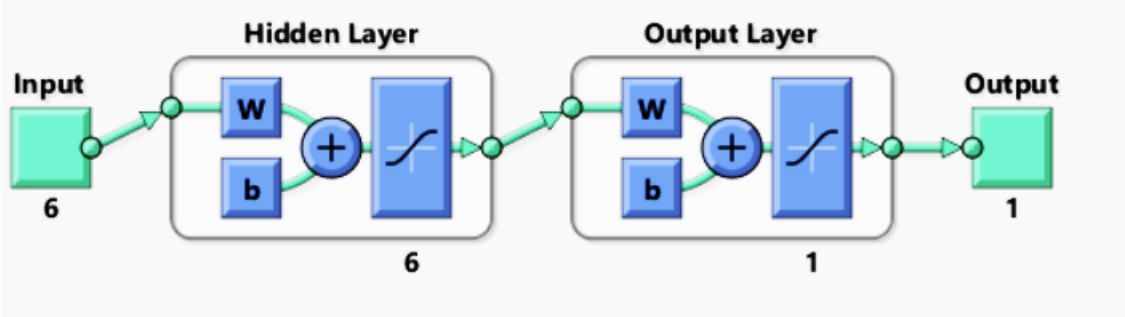

Figure 17. Number of layers used for modeling

A total of 182 data points were collected to develop a model for predicting the compressive strength of FC. The input variables for this study include binder content, natural fine aggregate, water, foaming agent, and age of testing of the specimen. The output variable being measured is the compressive strength [106]. The table presented in Figure 7 illustrates the input and output variables utilized in the ANN analysis for determining the compressive strength of FC.

Table 7. Variables used for ANN analysis to determine the compressive strength of FC

	Binder content (kg/m^3)	Natural Fine Aggregate (kg/m^3)	Water (kg/m^3)	Foaming agent (kg/m^3)	Age of Testing (Days)	Compressive Strength (MPa)
Maximum	600.00	1355.00	484.00	0.17	3.00	0.10
Minimum	107.20	0.00	68.90	60.00	180.00	18.50

Prior to making predictions, the data undergoes pre-processing utilizing normalization techniques. This is done to ensure that the data is evenly distributed within the range of -1 to +1. It is essential to incorporate normalization methods in the pre-processing of data for machine learning. These techniques are employed to transform data into a format that can be easily processed by machine learning algorithms. Normalization can enhance the performance of machine learning models by mitigating the impact of outliers, expediting convergence, and reducing overfitting. The normalization technique utilized in this modeling is demonstrated in Equation (1), specifically employing a scaling technique.

$$X_N = \left\{\left[\frac{2(X - X_{min})}{(X_{Max} - X_{Min})}\right] - 1\right\} \quad (1)$$

Whereas X_N is the normalized data value, X_{min} is the minimum value of the observed data and X_{max} is the maximum value of observed data from the literature. Levenberg Marquardt (LM) algorithm with transform function as TANSINGH is used to predict the compressive strength. A popular optimization method for training ANN is the LM algorithm. It is frequently applied to the resolution of nonlinear regression issues, including forecasting concrete's compressive strength. By minimizing the difference between the predicted output and the actual output for each input-output combination in the training data, the LM algorithm is used to optimize the weights and biases of the ANN. The weights and biases in the network are modified iteratively, guided by the error between the expected output and the actual output. Feedforward propagation method with performance error as mean square error was used in this study. A hyperparameter called "epochs" determines how many times the learning algorithm will go through the complete training dataset. Every sample in the training dataset has had a chance to change the internal model parameters once during an epoch. Epoch for the present study is shown in Figure 18.

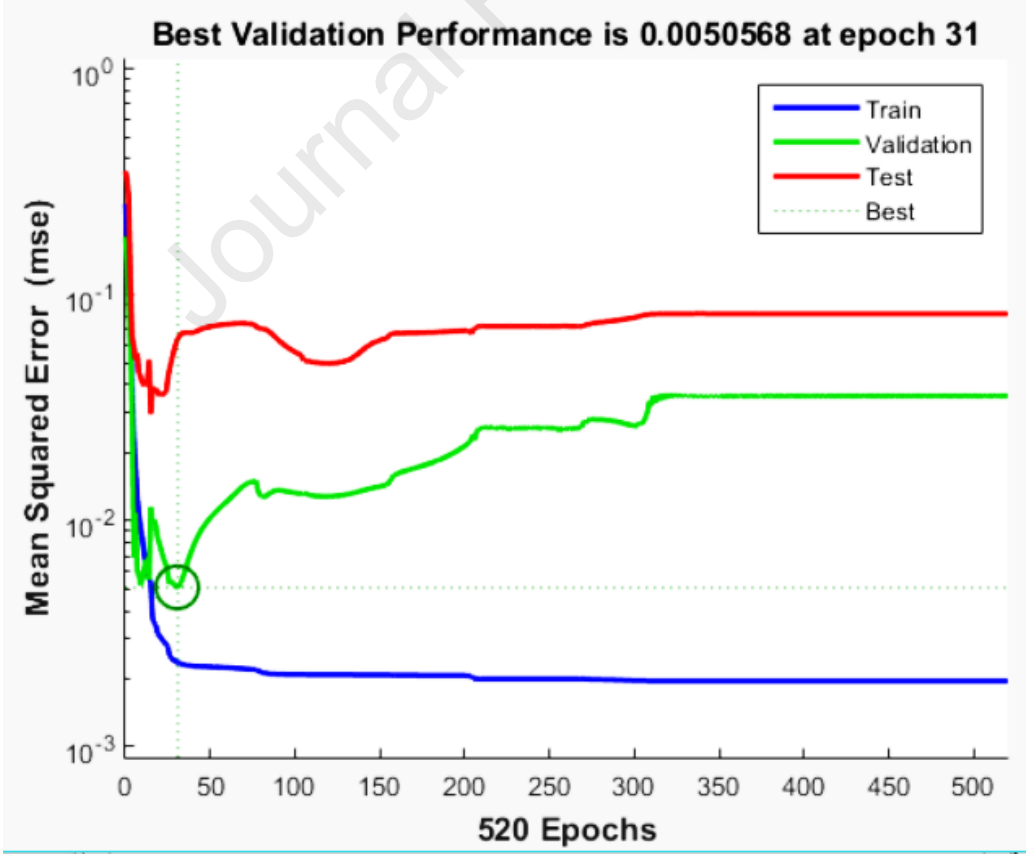

Figure 18. Epochs for ANN model to predict the compressive strength

The literature data utilized *k*-fold cross-validation, where the data was divided into ten subsets of approximately equal size. The neural network was trained using a total of seven sets, which accounted for 70% of the observations. The remaining three sets, comprising 30% of the observations, were set aside for evaluating the effectiveness of the model. The procedure was repeated ten times to accommodate the ten sets of data. Seven sets were utilized for model development, while the remaining three sets were used for testing purposes. This was done using four distinct combinations. The utilization of this method offers the advantage of enabling the anticipation of the overall predictive capability of the ANN). The *k-fold* cross-validation method, specifically using k =10 folds, is a widely employed technique for obtaining accurate data models. The coefficient of determination (R2) was utilized to evaluate the performance of the model illustrated in Figure 19 for k = 1 cross-fold cross-validation. The number of neurons has been set to 7, which corresponds to the number of input variables. Additionally, two hidden layers have been utilized, with one serving as the input layer and the other as the output layer. Based on the findings presented in Figure 20, it can be concluded that the optimal value for k -fold cross-validation is determined to be k = 1. This particular value exhibits the highest average R-squared score of 0.921 for both training and testing.

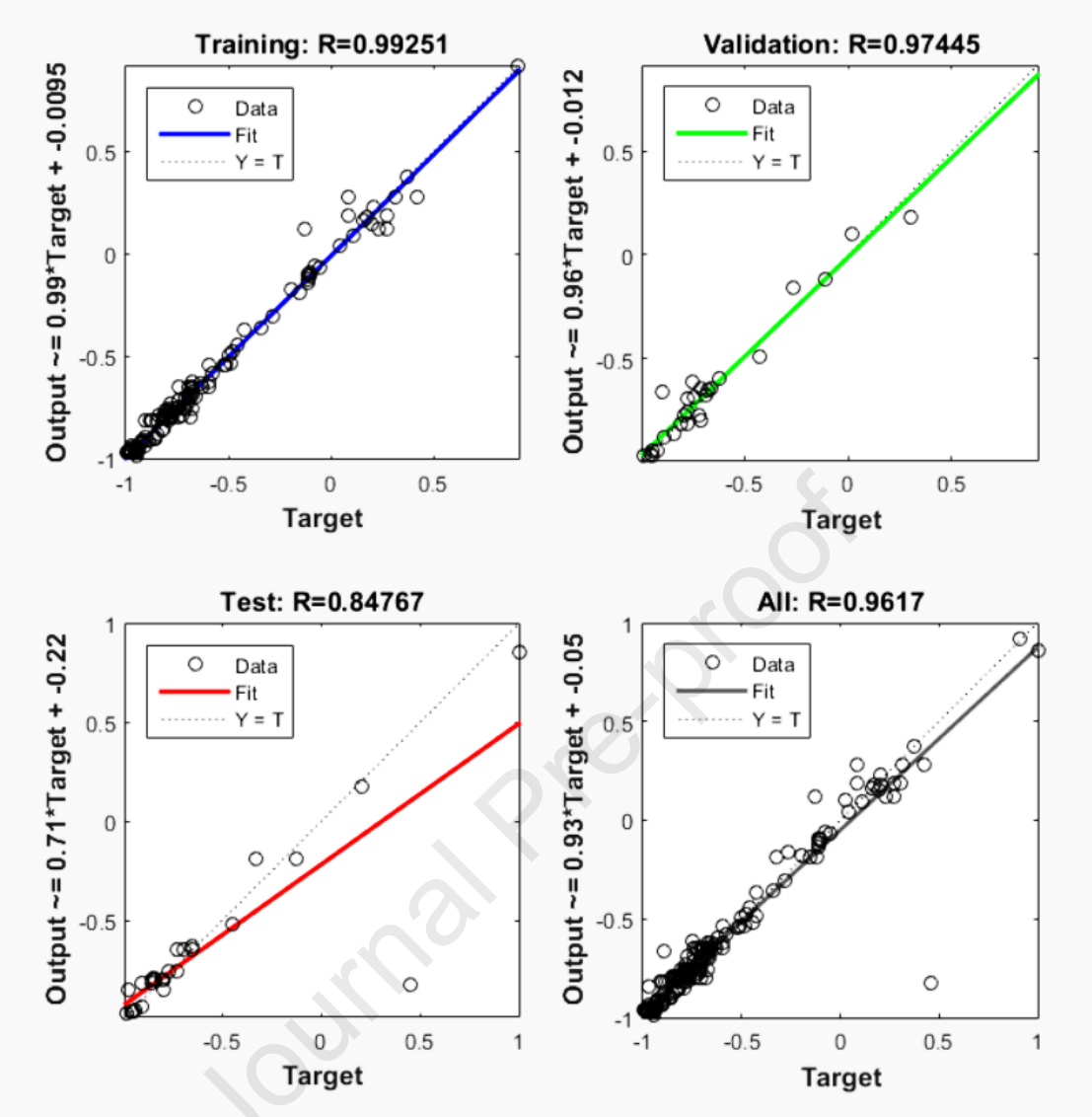

Figure 19. Performance of ANN model (*k*=1) to predict compressive strength

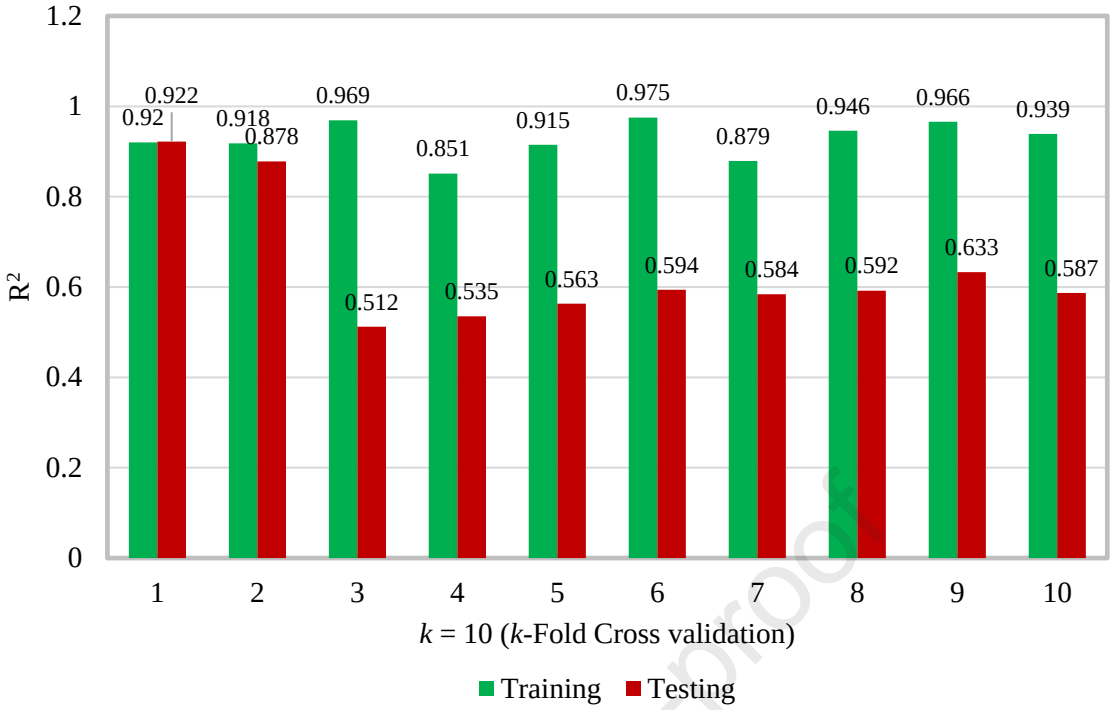

Figure 20. *k*-fold (*k*=1) cross-validation method for the ANN model

The figure provided in Figure 20 displays the predicted compressive strength for the CCNP blended FC. It has been determined that the input parameters exhibit a significant relationship. The predicted compressive strength was determined by utilizing the weights and biases obtained through the implementation of the ANN technique. Equation (9) is utilized for the estimation of the normalized compressive strength (MPa), while the denormalized value is obtained. Equations (2) through (8) are utilized for the estimation of the constant value ranging from E1 to E7.

E1 = 2.8561 x tanh[(Bn x 0.53035) + (Sn x 0.49116) - (Wn x 0.40621) – (FAn x 2.3467) + (Dn x 2.1055) + (ATn x 0.87196) – 2.4344] (2)

E2 = 1.4268 x tanh [(Bn x 2.56652) + (Sn x 5.6652) – (Wn x 1.0366) + (FAn x 2.4696) – (Dn x 2.2601) + (ATn x 1.5209) + 0.15534] (3)

E3 = -2.1366 x tanh [(Bn x 1.3085) + (Sn x 0.35256) – (Wn x 1.1101) + (FAn x 0.50655) + (Dn x 0.75319) – (ATn x 0.17218) – 0.0027526] (4)

E4 = 0.84238 x tanh [(Bn x 2.9477) – (Sn x 2.2667) + (Wn x 0.34965) + (FAn x 0.97791) – (Dn x 0.011495) + (ATn x 0.66825) – 0.077919] (5)

$$E5 = 2.4435 \times \tanh [(Bn \times 0.40747) + (Sn \times 0.58673) – (Wn \times 1.0959) + (FAn \times 2.6042) – (Dn \times 1.3285) – (ATn \times 1.1623) + 2.2803] \quad (6)$$

$$E6 = -1.7148 \times \tanh [(Bn \times 0.31346) + (Sn \times 3.4977) + (Wn \times 1.3966) – (FAn \times 0.71556) – (Dn \times 1.1189) – (ATn \times 1.4739) – 2.6024] \quad (7)$$

$$E7 = -1.2093 \times \tanh [-(Bn \times 2.6287) – (Sn \times 0.31735) + (Wn \times 0.13484) + (FAn \times 1.0637) – (Dn \times 2.0254) – (ATn \times 1.2057) – 2.589] \quad (8)$$

$$CSn = \tanh [(E1 + E2 + E3 + E4 + E5 + E6 + E7) – 1.7211] \quad (9)$$

where,

Bn – Normalized binder content (kg/m^3)

Sn – Normalized fine Aggregate content or normalized sand content (kg/m^3)

Wn – Normalized water content (kg/m^3)

FAn – Normalized foaming agent content (kg/m^3)

Dn – Normalized density content of FC (kg/m^3)

ATn – Normalized Age of Testing of specimen (days)

CSn – Normalized compressive strength of FC (MPa)

6. Conclusions

The utilization of nanoparticles in FC is currently in the exploratory phase, and the implementation of these particles in construction applications is currently limited. It is certainly probable that nanoparticles have the potential to enhance the physical, mechanical, and durability properties of the FC. This study aimed to examine the potential application of different weight fractions (ranging from 1% to 6%) of CCNP in FC for improving physical and mechanical properties. The present study yields the following conclusions:

- The increase in the weight percentage of CCNP resulted in a decrease in the slump flow of FC. The workability of FC is adversely affected by the significant specific surface area of CCNP.
- The inclusion of CCNP in FC leads to improved compressive, tensile, and flexural strengths. The recommended weight fraction of CCNP to be incorporated into FC is 4%. The use of CCNP enhances the strength characteristics of FC by promoting the formation of a more compact structure of hydration products. This results in improved particle volume distribution and a reduction in pore size and interconnectivity.
- The inclusion of more than 4% CCNP in FC leads to particle clumping and agglomeration, which is caused by non-uniform dispersion. This ultimately leads to a reduction in mechanical properties.
- The increase in CCNP weight fraction led to an improvement in the FC's porosity as well as reduced its capacity to absorb water. The high reactivity of the material leads to a decrease in water absorption and permeable porosity. This is achieved by increasing the density of the interfacial transition zone.
- Development of correlation of the mechanical properties of FC-CCNP is proposed in this study.
- Estimation of compressive strength (output variable) from seven ingredients (input variables) of FC, using *k*-fold-cross validation (*k*=1) with the best R-squared value as 0.921.

The incorporation of CCNP into FC leads to an increase in density, thus improving the mechanical and durability properties. This observation is supported by the examination of morphological characteristics.

Funding

The research was funded by the Ministry of Higher Education (MoHE) of Malaysia under the Fundamental Research Grant Scheme (FRGS) (FRGS/1/2022/TK01/USM/02/3).

Conflicts of Interest

The authors declare no conflict of interest.

References

1. Monteiro H, Moura B, Soares N. Advancements in nano-enabled cement and concrete: Innovative properties and environmental implications. J. Build. Eng. 2022;56;104736.
2. Nawi MNM, Lee A, Mydin MAO, Osman, W.N. , Rofie, M.K. Supply chain management (SCM): Disintegration team factors in Malaysian Industrialised Building System (IBS) construction projects. Int. J. Supply Chain Manag. 2018, 7(1), 140-143.
3. Mydin MAO, Phius AF, Sani NM, Tawil NM. Potential of Green Construction in Malaysia: Industrialised Building System (IBS) vs Traditional Construction Method. E3S Web Conf. 2014;3;01009.
4. Gemi, L., Alsdudi, M., Aksoylu, C., Yazman, Ş., Özkılıç, Y. O., & Arslan, M. H. (2022). Optimum amount of CFRP for strengthening shear deficient reinforced concrete beams. Steel and Composite Structures.
5. Özkılıç, Y. O., Aksoylu, C., & Arslan, M. H. (2021). Numerical evaluation of effects of shear span, stirrup spacing and angle of stirrup on reinforced concrete beam behaviour. Structural Engineering and Mechanics, An Int'l Journal, 79(3), 309-326.
6. Başaran, B., Aksoylu, C., Özkılıç, Y. O., Karalar, M., & Hakamy, A. (2023, August). Shear behaviour of reinforced concrete beams utilizing waste marble powder. In Structures (Vol. 54, pp. 1090-1100). Elsevier.
7. Özkılıç, Y. O., Başaran, B., Aksoylu, C., Karalar, M., & Martins, C. H. (2023). Mechanical behavior in terms of shear and bending performance of reinforced concrete beam using waste fire clay as replacement of aggregate. Case Studies in Construction Materials, 18, e02104.
8. Yıldızel, S. A., Özkılıç, Y. O., Bahrami, A., Aksoylu, C., Başaran, B., Hakamy, A., & Arslan, M. H. (2023). Experimental Investigation and Analytical Prediction of Flexural Behaviour of Reinforced Concrete Beams with Steel Fibres Extracted from Waste Tyres. Case Studies in Construction Materials, e02227.
9. Ganesan S, Othuman Mydin MA, Sani NM, Che Ani AI. Performance of polymer modified mortar with different dosage of polymeric modifier. MATEC Web Conf. 2014;15;01039.
10. Mohamad N, Iman MA, Othuman Mydin MA, Samad AAA, Rosli JA, Noorwirdawati A. Mechanical properties and flexure behaviour of lightweight foamed concrete incorporating coir fibre. IOP Conf. Ser. Earth Environ. Sci. 2018;140;012140.
11. Huang, H., Li, M., Yuan, Y., & Bai, H. (2022). Theoretical analysis on the lateral drift of precast concrete frame with replaceable artificial controllable plastic hinges. Journal of Building Engineering, 62, 105386. doi: https://doi.org/10.1016/j.jobe.2022.105386
12. Mohamad N, Samad, AAA, Lakhiar MT, Othuman Mydin MA, Jusoh S, Sofia A, Efendi SA. Effects of Incorporating Banana Skin Powder (BSP) and Palm Oil Fuel Ash (POFA) on Mechanical Properties of Lightweight Foamed Concrete. Int. J. Int. Eng. 2018;10;169-176.

13. Serri E, Suleiman MZ, Mydin MAO. The effects of oil palm shell aggregate shape on the thermal properties and density of concrete. Adv. Mat. Res. 2014;935;172-175.

14. Zhang, W., Liu, X., Huang, Y., & Tong, M. (2022). Reliability-based analysis of the flexural strength of concrete beams reinforced with hybrid BFRP and steel rebars. Archives of Civil and Mechanical Engineering, 22(4), 171. doi: 10.1007/s43452-022-00493-7

15. Huang, H., Yuan, Y., Zhang, W., & Li, M. (2021). Seismic behavior of a replaceable artificial controllable plastic hinge for precast concrete beam-column joint. Engineering Structures, 245, 112848. doi: https://doi.org/10.1016/j.engstruct.2021.112848S

16. Sun, L., Wang, C., Zhang, C., Yang, Z., Li, C.,... Qiao, P. (2022). Experimental investigation on the bond performance of sea sand coral concrete with FRP bar reinforcement for marine environments. Advances in Structural Engineering, 26(3), 533-546. doi: 10.1177/13694332221131153

17. Chang, Q., Liu, L., Farooqi, M. U., Thomas, B., & Özkılıç, Y. O. (2023). Data-driven based estimation of waste-derived ceramic concrete from experimental results with its environmental assessment. Journal of Materials Research and Technology, 24, 6348-6368.

18. Özkılıç, Y. O., Karalar, M., Aksoylu, C., Beskopylny, A. N., Stel'makh, S. A., Shcherban, E. M., ... & Azevedo, A. R. (2023). Shear performance of reinforced expansive concrete beams utilizing aluminium waste. Journal of Materials Research and Technology, 24, 5433-5448.

19. Wang, M., Yang, X., & Wang, W. (2022). Establishing a 3D aggregates database from X-ray CT scans of bulk concrete. Construction and Building Materials, 315, 125740. doi: https://doi.org/10.1016/j.conbuildmat.2021.125740S

20. Zhang, W., Kang, S., Liu, X., Lin, B., & Huang, Y. (2023). Experimental study of a composite beam externally bonded with a carbon fiber-reinforced plastic plate. Journal of Building Engineering, 71, 106522. doi: https://doi.org/10.1016/j.jobe.2023.106522S

21. Fang, B., Hu, Z., Shi, T., Liu, Y., Wang, X., Yang, D.,... Zhao, Z. (2022). Research progress on the properties and applications of magnesium phosphate cement. Ceramics International. doi: https://doi.org/10.1016/j.ceramint.2022.11.078

22. Tao Shi, Y. L. Z. H. Deformation Performance and Fracture Toughness of Carbon Nanofiber Modified Cement-Based Materials. ACI Materials Journal, 119(5). doi: 10.14359/51735976

23. Shi, T., Liu, Y., Zhao, X., Wang, J., Zhao, Z., Corr, D. J.,... Shah, S. P. (2022). Study on mechanical properties of the interfacial transition zone in carbon nanofiber-reinforced cement mortar based on the PeakForce tapping mode of atomic force microscope. Journal of Building Engineering, 61, 105248. doi: https://doi.org/10.1016/j.jobe.2022.105248

24. Tu, H., Wei, Z., Bahrami, A., Kahla, N. B., Ahmad, A., & Özkılıç, Y. O. (2023). Recent advancements and future trends in 3D printing concrete using waste materials. Developments in the Built Environment, 100187.

25. Zhou, S., Lu, C., Zhu, X., & Li, F. (2021). Preparation and Characterization of High-Strength Geopolymer Based on BH-1 Lunar Soil Simulant with Low Alkali Content. Engineering, 7(11), 1631-1645. doi: https://doi.org/10.1016/j.eng.2020.10.016

26. Rudnai G. Lightweight Concretes. Akademikiado: Budapest, Hungary; 1963.

27. Liu Y, Wang L, Cao K, Sun L. Review on the Durability of Polypropylene Fibre-Reinforced Concrete. Adv. Civ. Eng. 2021;6652077.

28. Pakravan HR, Latifi M, Jamshidi M. Hybrid short fiber reinforcement system in concrete: A Review. Constr. Build. Mater. 2017;142;280-294.

29. Tambichik MA, Abdul Samad AA, Mohamad N, Mohd Ali AZ, Othuman Mydin MA, Mohd Bosro MZ, Iman MA. Effect of combining Palm Oil Fuel Ash (POFA) and Rice Husk Ash (RHA) as partial cement replacement to the compressive strength of concrete. Int. J. Integr. Eng., 2018;10;61-67.

30. Awang H, Mydin MAO, Roslan AF. Effects of fibre on drying shrinkage, compressive and flexural strength of lightweight foamed concrete. Adv. Mat. Res. 2012;587;144-149.

31. Mydin MAO, Soleimanzadeh S. Effect of polypropylene fiber content on flexural strength of Lightweight foamed concrete at ambient and elevated temperatures. Adv. Appl. Sci. Res. 2012;3;2837-2846.

32. Ahmed HK, Abbas WA, AlSaff D. Effect of Plastic Fibers on Properties of Foamed Concrete. Eng. Technol. J. 2013;31,1313-1330.

33. Castillo-Lara, JF, Flores-Johnson EA, Valadez-Gonzalez A, Herrera-Franco PJ, Carrillo JG, Gonzalez-Chi PI, Li QM. Mechanical Properties of Natural Fiber Reinforced Foamed Concrete. Materials 2020;13;3060.

34. Falliano D, de Domenico D, Ricciardi G, Gugliandolo E. Compressive and flexural strength of fiber-reinforced foamed concrete: Effect of fiber content, curing conditions and dry density. Constr. Build. Mater. 2019;198;479-493.

35. Othuman Mydin MA, Mohd Zamzani N. Coconut fiber strengthen high performance concrete: Young's modulus, ultrasonic pulse velocity and ductility properties. International Journal of Engineering and Technology (UAE), 2018;7(2);284-287.

36. Nensok MH, Mydin MAO, Awang H. Investigation of Thermal, Mechanical and Transport Properties of Ultra Lightweight Foamed Concrete (UFC) Strengthened with Alkali Treated Banana Fibre. J. Adv. Res. Fluid Mech. Therm. Sci., 2021;86(1);123-139.

37. Brostow W, Hagg Lobland HE. Materials: Introduction and Applications. John Wiley & Sons; 2017.

38. Song N, Li Z, Yi W, Wang S. Properties of foam concrete with hydrophobic starch nanoparticles as foam stabilizer. J. Build. Eng. 2022,56;104811.

39. Serri E, Othuman Mydin MA, Suleiman MZ. The influence of mix design on mechanical properties of oil palm shell lightweight concrete. J. Mater. Environ. Sci. 2015;6(3);607-612.

40. Suhaili SS, Mydin MAO, Awang H. Influence of Mesocarp Fibre Inclusion on Thermal Properties of Foamed Concrete. J. Adv. Res. Fluid Mech. Therm. Sci. 2021;87(1);1-11.

41. Gajanan K, Tijare, S. Applications of nanomaterials. Mater. Today Proc. 2018;5;1093-1096.

42. Madenci, E., Özkılıç, Y. O., Aksoylu, C., Asyraf, M. R. M., Syamsir, A., Supian, A. B. M., & Elizaveta, B. (2023). Experimental and Analytical Investigation of Flexural Behavior of Carbon Nanotube Reinforced Textile Based Composites. Materials, 16(6), 2222.

43. Madenci, E., Özkılıç, Y. O., Aksoylu, C., Asyraf, M. R. M., Syamsir, A., Supian, A. B. M., & Mamaev, N. (2023). Buckling Analysis of CNT-Reinforced Polymer Composite Beam Using Experimental and Analytical Methods. Materials, 16(2), 614.

44. Madenci, E., Özkılıç, Y. O., Hakamy, A., Tounsi, A. (2023). Experimental tensile test and micro-mechanic investigation on carbon nanotube reinforced carbon fiber composite beams. Advances in Nano Research 14(5). 10.12989/anr.2023.14.5.443

45. Alhassan M, Alkhawaldeh A, Betoush N, Alkhawaldeh M, Huseien GF, Amaireh L, Elrefae A. Life Cycle Assessment of the Sustainability of Alkali-Activated Binders. Biomimetics 2023;8(1);58.

46. Mydin MAO, Nawi MNM, Omar R, Mohamed Amine K, Ali IM, Deraman R. The use of inorganic ferrous–ferric oxide nanoparticles to improve fresh and durability properties of foamed concrete. Chemosphere. 2023;317;137661.

47. He X, Shi X. Chloride Permeability and Microstructure of Portland Cement Mortars Incorporating Nanomaterials. Transp. Res. Rec. J. Transp. Res. Board 2008;2070;13-21.

48. Chang TP, Shih, JY, Yang KM, Hsiao TC. Material properties of portland cement paste with nano-montmorillonite. J. Mater. Sci. 2007;42;7478-7487.

49. Dhiman NK, Sidhu N, Agnihotri S, Mukherjee A, Reddy MS. Role of nanomaterials in protecting building materials from degradation and deterioration. Biodegrad. Biodeterior. Nanoscale 2022;405-475.

50. Irshidat MR, Al-Saleh MH. Thermal performance and fire resistance of nanoclay modified cementitious materials. Constr. Build. Mater. 2018;159;213-219.

51. Nehdi ML. Clay in cement-based materials: Critical overview of state-of-the-art. Constr. Build. Mater. 2014;51;372-382.

52. Hou L, Li J, Lu Z, Niu Y, Jiang J, Li T. Effect of nanoparticles on foaming agent and the foamed concrete. Constr. Build. Mater. 2019;227;116698.

53. Huang, Z.; Zhang, T.; Wen, Z. Proportioning and characterization of Portland cement-based ultra-lightweight foam concretes. Constr. Build. Mater. 2015, 79, 390–396.

54. Du, H.J.; Du, S.H.; Liu, X.M. Durability performances of concrete with nano-silica. Constr. Build. Mater. 2014, 73, 705–712.

55. Rong, Z, Sun W, Xiao H, Jiang G. Effects of nano-SiO2 particles on the mechanical and microstructural properties of ultra-high performance cementitious composites. Cem. Concr. Compos. 2015;56;25-31.

56. Norhasri MM, Hamidah M, Fadzil AM. Applications of using nano material in concrete: A review. Constr. Build. Mater. 2017;133;91-97.

57. Gokçe HS, Hatungimana D, Ramyar K. Effect of fly ash and silica fume on hardened properties of foamed concrete. Constr. Build. Mater. 2019;194;1-11.

58. Zhang YQ, Chang ZD, Luo WL, Gu SN, Li WJ, An, J.B. An effect of starch particles on foam stability and dilational viscoelasticity of aqueous-foam. Chin. J. Chem. Eng. 2015;23;276-280.

59. Liu X, Chen L, Liu A, Wang X. Effect of Nano-CaCO3 on Properties of Cement Paste. Energy Procedia 2012;16;991-996.

60. Seifan M, Mendoza S, Berenjian A. Mechanical properties and durability performance of fly ash based mortar containing nano and micro-silica additives. Constr. Build. Mater. 2020;252;119121.

61. Othuman Mydin MA, Mohd Nawi, MN, Mohamed O, Sari MW. Mechanical Properties of Lightweight Foamed Concrete Modified with Magnetite (Fe3O4) Nanoparticles. Materials. 2022;15(17);5911.

62. Adak D, Sarkar, M, Mandal S. Effect of nano-silica on strength and durability of fly ash based geopolymer mortar. Constr. Build. Mater. 2014;70;453-459.

63. Poudyal L. Use of Nanotechnology in Concrete. Master's Thesis. Texas Tech University, Lubbock, TX, USA; 2018.

64. Shah SP, Hou P, Konsta-Gdoutos MS. Nano-modification of cementitious material: Toward a stronger and durable concrete. J. Sustain. Cem. Mater. 2015;5;1-22.

65. Batuecas E, Liendo, F, Tommasi T, Bensaid S, Deorsola F, Fino D. Recycling CO2 from flue gas for CaCO3 nanoparticles production as cement filler: A Life Cycle Assessment. J. CO2 Util. 2021;45;101446.

66. Poudyal L, Adhikari K, Won M. Mechanical and durability properties of portland limestone cement (PLC) incorporated with nano calcium carbonate (CaCO3). Materials 2021;14;905.

67. Poudyal L, Adhikari K. Environmental sustainability in cement industry: An integrated approach for green and economical cement production. Resour. Environ. Sustain. 2021;4;100024.

68. BS EN 197-1. Cement - Composition, specifications and conformity criteria for common cements. British Standards Institute: London, UK; 2011.

69. ASTM C33-03. Standard Specification for Concrete Aggregates. American Society for Testing and Materials. West Conshohocken, PA: ASTM International; 2003.

70. ASTM C128-15. Standard Test Method for Relative Density (Specific Gravity) and Absorption of Fine Aggregate. American Society for Testing and Materials. West Conshohocken, PA: ASTM International; 2015.

71. BS EN 3148. Water for Making Concrete (Including Notes on the Suitability of the Water). British Standards Institute: London, UK; 1980.

72. Mydin MAO, Nawi MNM, Munaaim MAC, Mohamad N, Samad AAA, Johari I. Effect of steel fibre volume fraction on thermal performance of Lightweight Foamed Mortar (LFM) at ambient temperature. J. Adv. Res. Fluid Mech. Therm. Sci., 2018;47(1);119-126.

73. ASTM C1437-20. Standard Test Method for Flow of Hydraulic Cement Mortar. American Society for Testing and Materials. West Conshohocken, PA: ASTM International; 2020.

74. BS EN 12390-5. Testing Hardened Concrete. Flexural Strength of Test Specimens. British Standards Institute: London, UK; 2019

75. BS EN 12390-3. Testing Hardened Concrete. Compressive Strength of Test Specimens. British Standards Institute: London, UK; 2011.

76. BS EN 12390-6. Testing Hardened Concrete. Tensile Splitting Strength of Test Specimens. British Standards Institute: London, UK, 2009.

77. Amran Y, Farzadnia N, Abang Ali A. Properties and applications of foamed concrete; a review. Constr Build Mater. 2015;101;990-1005.

78. BS EN 1881-122. Testing concrete Method for determination of water absorption. British Standards Institute: London, UK; 2020.

79. ASTM C878/C878M-22. Standard Test Method For Restrained Expansion Of Shrinkage-Compensating Concrete. American Society for Testing and Materials. West Conshohocken, PA: ASTM International; 2022.

80. ASTM C 230-97. Flow Table for Use in Tests of Hydraulic Cement. American Society for Testing and Materials. West Conshohocken, PA: ASTM International; 1997.

81. Supit SWM, Shaikh FUA. Durability properties of high volume fly ash concrete containing nano-silica. Materials and Structures. 2015;48(8);2431-2445.

82. Meng T, Qian KL, Qian XQ. Effect of composite nano-addition on mechanics strength and microstructure of cement paste. Rare Metal Materials and Engineering. 2008;37;631-633.

83. Othuman Mydin MA, Evaluation of the Mechanical Properties of Lightweight Foamed Concrete at Varying Elevated Temperatures. Fire. 2023;6(2);53.

84. Nensok, MH, Mydin MAO, Awang H. Fresh state and mechanical properties of ultra-lightweight foamed concrete incorporating alkali treated banana fibre. J. Teknol., 2022;84(1);117-128.

85. Musa, M. , Othuman Mydin, M.A. , Abdul Ghani, A.N. Influence of oil palm empty fruit bunch (EFB) fibre on drying shrinkage in restrained lightweight foamed mortar. Int. J. of Innov. Technol. and Exp. Eng., 2019, 8(10), pp. 4533–4538.

86. Ganesan, S.; Othuman Mydin, M. A.; Mohd Yunos, M. Y.; Mohd Nawi, M. N. Thermal Properties of Foamed Concrete with Various Densities and Additives at Ambient Temperature. Appl. Mech. Mater. 2015, 747, 230-233.

87. Nazari A, Riahi S, Shirin R, Seyedeh FS, Khademno, A. The effects of incorporation Fe2O3 nano particles on tensile and flexural strength of concrete. J. Am. Sci. 2010;6;90-93.

88. Hakamy A. Effect of CaCO3 nanoparticles on the microstructure and fracture toughness of ceramic nanocomposites. Journal of Taibah University for Science. 2020;14(1);1201-1207.

89. Liu X, Wang X, Liu, A. Study on the mechanical properties of cement modified by nanoparticles. Applied mechanics materials. 2012;157-158;161-164.

90. Shaikh FU, Supit, SWM. Mechanical and durability properties of high volume fly ash concrete containing calcium carbonate nanoparticles. Construction and building materials. 70;2014; 309-321.

91. Mansi A, Sor NH, Hilal N, Qaidi SMA. The Impact of Nano Clay on Normal and High-Performance Concrete Characteristics: A Review. IOP Conf. Ser. Earth Environ. Sci. 2022;961;012085.

92. Han B, Li Z, Zhang L, Zeng S, Yu X, Han B, Ou J. Reactive powder concrete reinforced with nano SiO2-coated TiO2. Constr. Build. Mater. 2017;148;104-112.

93. Mohammed A, Rafiq S, Mahmood W, Al-Darkazalir H, Noaman R, Qadir W, Ghafor K. Artificial Neural Network and NLR techniques to predict the rheological properties and compression strength of cement past modified with nanoclay. Ain Shams Eng. J. 2021;12;1313-1328.

94. Nejad FM, Tolouei M, Nazari H, Naderan A. Effects of calcium carbonate nanoparticles and fly ash on mechanical and permeability properties of concrete. Advances in civil engineering materials. 2018;7(1);651-668.

95. Emamian SA, Eskandari-Naddaf, H. Effect of porosity on predicting compressive and flexural strength of cement mortar containing micro and nano-silica by ANN and GEP. Constr. Build. Mater. 2019;218;8-27.

96. Martinez-Garcia R., Sanchez de Rojas MI, Jagadesh P, Lopez-Gayarre F, Moran-del-Pozo JM, Juan-Valdes A. Effects of pores on the mechanical and durability properties on high strength recycled fine aggregate mortar. Case Studies in Construction Materials. 2022;16;e01050.

97. Roslan AF, Awang H, Mydin MAO. Effects of various additives on drying shrinkage, compressive and flexural strength of lightweight foamed concrete. Advanced Materials Research. 2013;626;594-604.

98. Abellan-Garcia J, Iqbal Khan M, Abbas YM, Martínez-Lirón V, Carvajal-Muñoz JS. The drying shrinkage response of recycled-waste-glass-powder-and calcium-carbonate-based ultrahigh-performance concrete. Constr. Build. Mater. 2023, 131163.

99. Ni K, Shi Y, Hu Z, Zhang Y, Wan P. Effect of Coal Gangue Grain Size on Strength of Foam Concrete. Journal of Physics: Conference Series. 2020;1635;012080.

100. Xiao J, Zhang H, Zou S, Duan Z, Ma Y. Developing recycled foamed concrete for engineered material arresting system. J. Build. Eng. 2022;53;104555.

101. Serudin AM, Mydin MAO, Ghani ANA. Influence of Fibreglass Mesh on Physical Properties of Lightweight Foamcrete. IIUM Engineering Journal. 2021;22(1);23-34.

102. Jagadesh P, Nagarajan V, Karthik Prabhu T, Karthik Arunachalam K. Effect of nano titanium di oxide on mechanical properties of fly ash ad ground granulated blast furance slage based geopolymer concrete. Journal of Building Engineering. 2022;61;105235.

103. Ramezanianpour AA, Ghiasvand E, Nickseresht L, Mahdikhani M, Moodi F. Influence of various amounts of limestone powder on the performance of Portland limestone cement concretes. Cement concrete composites. 2009;31;715-720.

104. Martinez-Garcia R, Jagadesh P, Burdalo-Salcedo G, Palencia C, Fernandez-Raga M, Fraile-Fernandez FJ. Impact of design parameters on the ratio of compressive to spilt tensile strength of self-compacting concrete with recycled aggregate. Materials. 2021;14(13);3480.

105. Isleem HF, Jagadesh P, Ahmad J, Qaidi SMA, Althoey F., Najm HM, Sabri MM. Finite element and analytical modelling of PVC-confined concrete columns under axial compression. Frontiers in materials, 2022;9;1011675.

106. Tikalsky PJ, Pospisil J, MacDonald W. A method for assessment of the freeze–thaw resistance of preformed foam cellular concrete. Cement and Concrete Research. 2004;34(5);889-893.

Declaration of interests

☒ The authors declare that they have no known competing financial interests or personal relationships that could have appeared to influence the work reported in this paper.

☐The authors declare the following financial interests/personal relationships which may be considered as potential competing interests: